Journal of Molecular Structure 1058 (2014) 79–96

Contents lists available at ScienceDirect

Journal of Molecular Structure

journal homepage: www.elsevier.com/locate/molstruc

Monomeric and dimeric structures analysis and spectroscopic characterization of 3,5-difluorophenylboronic acid with experimental (FT-IR, FT-Raman, ^{1}H and ^{13}C NMR, UV) techniques and quantum chemical calculations

Mehmet Karabacak [a], Etem Kose [b], Ahmet Atac [b], Abdullah M. Asiri [c,d], Mustafa Kurt [e,*]

[a] Department of Mechatronics Engineering, HFT Technology Faculty, Celal Bayar University, Turgutlu, Manisa, Turkey
[b] Department of Physics, Celal Bayar University, Manisa, Turkey
[c] Department of Chemistry, Faculty of Science, King Abdulaziz University, Jeddah, Saudi Arabia
[d] Center of Excellence for Advanced Materials Research, King Abdulaziz University, Jeddah, Saudi Arabia
[e] Department of Physics, Ahi Evran University, Kırsehir, Turkey

HIGHLIGHTS

- Molecular structure of 3,5-difluorophenylboronic acid conformers and its dimer structure were investigated.
- Spectroscopic properties of 3,5-difluorophenylboronic acid were examined.
- The complete assignments were performed on the basis of the total energy distribution (TED).
- TDOS, PDOS and OPDOS were investigated.

ARTICLE INFO

Article history:
Received 29 August 2013
Received in revised form 7 October 2013
Accepted 28 October 2013
Available online 4 November 2013

Keywords:
3,5-Difluorophenylboronic acid
Hydrogen-bonded dimer
DFT
FT-IR and FT-Raman spectra
UV and NMR spectra
HOMO–LUMO

ABSTRACT

The spectroscopic properties of 3,5-difluorophenylboronic acid (3,5-DFPBA, $C_6H_3F_2B(OH)_2$) were investigated by FT-IR, FT-Raman UV–Vis, ^{1}H and ^{13}C NMR spectroscopic techniques. FT-IR (4000–400 cm^{-1}) and FT-Raman spectra (3500–10 cm^{-1}) in the solid phase and ^{1}H and ^{13}C NMR spectra in DMSO solution were recorded. The UV spectra that dissolved in ethanol and water were recorded in the range of 200–400 nm for each solution. The structural and spectroscopic data of the molecule have been obtained for possible three conformers from DFT (B3LYP) with 6-311++G(d,p) basis set calculations. The geometry of the molecule was fully optimized, vibrational spectra were calculated and fundamental vibrations were assigned on the basis of the total energy distribution (TED) of the vibrational modes, calculated with scaled quantum mechanics (SQM) method and PQS program. Hydrogen-bonded dimer of title molecule, optimized by counterpoise correction, was also studied B3LYP at the 6-311++G(d,p) level and the effects of molecular association through O–H···O hydrogen bonding have been discussed. ^{1}H and ^{13}C NMR chemical shifts were calculated by using the gauge-invariant atomic orbital (GIAO) method. The electronic properties, such as excitation energies, oscillator strength, wavelengths, HOMO and LUMO energies, were performed by time-dependent density functional theory (TD-DFT) results complements with the experimental findings. Total and partial density of state (TDOS and PDOS) and also overlap population density of state (OPDOS) diagrams analysis were presented. The effects due to the substitutions of boric acid group and halogen were investigated. The results of the calculations were applied to simulate spectra of the title compound, which show excellent agreement with observed spectra. Besides, frontier molecular orbitals (FMO), molecular electrostatic potential (MEP), nonlinear optical properties (NLO) and thermodynamic features were performed.

© 2013 Elsevier B.V. All rights reserved.

1. Introduction

The boron and boronic acid recently have an importance increasing interest due to their extensive applications; such as potentials in the field of material science, supra molecular

* Corresponding author. Tel.: +90 386 211 45 54; fax: +90 386 252 80 54.
E-mail address: kurt@gazi.edu.tr (M. Kurt).

0022-2860/$ - see front matter © 2013 Elsevier B.V. All rights reserved.
http://dx.doi.org/10.1016/j.molstruc.2013.10.064

chemistry, analytical chemistry, medicine, biology, catalysis, organic synthesis and crystal engineering. A wide range of biologically importance of boronic acid derivatives have been synthesized as anti-metabolites [1–7]. Also boron-based compounds show preferential localization in tumor containing tissues making the boron-10 neutron capture therapy possible [8]. Boronic acid analogs were synthesized as transition state analogs for acyl transfer reactions [9] and inhibitors of dihydrotase [10]. The boronic acid moiety was also incorporated into amino acids and nucleosides as anti-tumor, anti-viral agents [11].

Because of their spectroscopic properties and chemical significance in particular, phenylboronic acid and its derivatives have been studied extensively by spectroscopic and theoretical methods. The crystal structure of phenylboronic acid was investigated by Rettig and Trotte [12]. The crystal structure of phenylboronic acid and its dimer were investigated experimentally using X-ray structural analysis and spectroscopic methods by Cyrański et al. [13]. Shimpi et al. [14] discussed crystal structures of 4-chloro and 4-bromophenylboronic acids and hydrates of 2- and 4-iodophenylboronic acid in two different forms, which were by single-crystal X-ray diffraction methods. The crystal structure of pentafluorophenylboronic acid molecule was investigated [15]. Wu et al. [16] and Bradley et al. [17] determined the crystal structures of 3-fluorophenylboronic acid and (2,6-difluoropheny) dihydroxyborane. The crystal structure of 3-aminophenylboronic acid monohydrate [18] and 3-formylphenylboronic acid [19] were reported. Rodríguez-Cuamatzi et al. [20,21] investigated the molecular structure of 1,4-Phenylenediboronic acid and 2,4-difluorophenylboronic acid. Infrared spectra of phenylboronic acid and diphenyl phenylboronate were studied by Faniran [22]. Theoretical and experimental analysis (DFT, FT-Raman, FT-IR and NMR) of 2-fluorophenylboronic acid were reported by Erdogdu et al. [23]. Kurt [24] investigated the molecular structure and vibrational spectra of the pentafluorophenylboronic acid and vibrational spectra of 4-chloro and 4-bromophenylboronic acids [25] by DFT and ab initio Hartree–Fock calculations. The experimental and theoretical study on the structures and vibrations of 3,4-dichlorophenylboronic acid were presented [26]. Kurt et al. presented an experimental and theoretical study of molecular structure and vibrational spectra of 3- and 4-pyridineboronic acid molecules [27] and molecular structure, vibrational spectroscopic studies and NBO analysis of the 3,5-dichlorophenylboronic acid were investigated by the density functional method [28]. Also the possible stable forms and molecular structures of 2,4-dimethoxy phenylboronic acid [29] (FT-IR, Raman and NMR) and 2,6-dimethoxy phenylboronic acid [30] were experimentally and theoretically studied using (FT-IR, Raman, NMR and XRD) spectroscopic methods. The experimental and theoretical investigation of the conformation, vibrational and electronic transitions of 2,3-difluorophenylboronic acid molecule [31] and acenaphthene-5-boronic acid [32] were published. Moreover Rani et al. [33] set out experimental and theoretical investigation of the conformation, vibrational and electronic transitions of methylboronic acid.

Recently, among the computational methods calculating the electronic structure of molecular systems, DFT calculations has been favorite one due to its great accuracy in reproducing the experimental values of molecular geometry, vibrational frequencies, atomic charges, dipole moment, thermo dynamical properties etc [23–42]. The DFT methods are increasingly used by spectroscopists for modeling these molecular properties.

The present work is a continuation of our previous study [31] and also the analysis of literature shows that no experimental and computational (DFT) spectroscopic study performed on the conformation, vibrational IR, Raman, NMR and UV spectra of the 3,5-DFPBA. Related to this phenomenon and inadequacy is observed in the literature, we wish to make this theoretical and experimental vibrational spectroscopic research based on the molecule to give a correct assignment of the fundamental bands in experimental FT-IR, FT-Raman, NMR and UV spectra and to present here electronic structure of the 3,5-DFPBA. In the ground state theoretical geometrical parameters, IR, Raman, NMR and UV spectra, HOMO–LUMO energies and MEP of title molecule were performed for the first time. A detailed interpretations of the vibrational spectra of the 3,5-DFPBA were made on the basis of the TED. Meticulous attention was focused on the effect of intermolecular O–H···O hydrogen bonding, modeled at the DFT/B3LYP level, on the bond distances, calculated frequencies and the infrared and Raman intensities, chemical shifts and excitation energies. Furthermore, various nonlinear optical properties of the 3,5-DFPBA molecule such as, the dipole moment, anisotropy of polarizability and first hyperpolarizability were also based on theoretical calculations. Moreover, the changes (the different temperatures in the thermodynamic functions (the heat capacity, entropy, and enthalpy) were investigated of title molecule. All results which examined by the experimental (IR, Raman, NMR and UV spectra) were supported by the computed results. Vibrational wavenumbers, absorption wavelengths, electronic properties and chemical shifts values are in fairly good agreement with the experimental results.

2. Experimental

The compound 3,5-DFPBA in solid state was purchased from Across Organics Company with a stated purity of 99% and it was used as such without further purification. The sample was prepared using a KBr disc technique because of solid state. The infrared spectrum of the title molecule was recorded between 4000 cm^{-1} and 400 cm^{-1} on a Perkin–Elmer FT-IR System Spectrum BX spectrometer. The spectrum was recorded at room temperature, with a scanning speed of 10 cm^{-1} min^{-1} and the spectral resolution of 4.0 cm^{-1}. FT-Raman spectrum of the molecule was recorded between 3500 cm^{-1} and 10 cm^{-1} on a Bruker RFS 100/S FT-Raman instrument using 1064 nm excitation from an Nd:YAG laser. The detector is a liquid nitrogen cooled Ge detector. Five hundred scans were accumulated at 4 cm^{-1} resolution using a laser power of 100 mW. The UV–Vis absorption spectrum of the 3,5-DFPBA is examined in the range 200–400 nm using Shimadzu UV-2101 PC, UV–Vis recording Spectrometer, solved in ethanol and water. Data are analyzed by UV PC personal spectroscopy software, version 3.91. NMR experiments were performed in Varian Infinity Plus spectrometer at 300 K. The compound was dissolved in DMSO. Chemical shifts were reported in ppm relative to tetramethylsilane (TMS) for ^{1}H and ^{13}C NMR spectra. NMR spectra were obtained at a base frequency of 150 MHz for ^{13}C and 600 MHz for ^{1}H nuclei.

3. Computational details

DFT calculations are important appliances for understanding the fundamental vibrational properties and the electronic structure of the compounds. Because of this reason, we have utilized the gradient corrected density functional theory (DFT) [43] with the Becke's three-parameter hybrid functional (B3) [44] for the exchange part and the Lee–Yang–Parr (LYP) correlation function [45], accepted as a cost-effective approach, for the computation of molecular structure, vibrational frequencies and energies of optimized structures by using Gaussian 09 suite of quantum chemical codes [46]. To determine conformational features of the molecule, the selected degree of torsional freedom, T (C–C–B–O), was varied from 0° to 360° in every 10° and the molecular energy profile was obtained with the B3LYP/6-311++G(d,p) method. In connection with the hydrogen atoms orientations of the oxygen atom of

boronic acid group, 3,5-DFBBA may has three possible conformations. The geometrical parameters including for three conformers of the 3,5-DFPBA and its hydrogen-bonded dimer in the ground state (in vacuum) were optimized at DFT by the hybrid B3LYP level of theory using the 6-311++G(d,p) basis set. After then the optimized structural parameters were used in the vibrational frequency, isotropic chemical shift and calculations of electronic properties. The vibrational frequencies, infrared and Raman intensities for the planar (C_s) structure of the most stable conformer of the title molecule were calculated. The computed harmonic frequencies were scaled factors in order to improve the agreement with the experimental results. In our study, we have followed two different scaling factors such as 0.983 up to 1700 cm^{-1} and 0.958 for greater than 1700 cm^{-1} [47,48].

The TED was calculated using the output files created at the end of the frequency calculations with the SQM method and PQS program [49,50] and the fundamental vibrational modes were characterized by their TED, which showed the relative contributions of the redundant internal coordinates to each normal vibrational mode of the molecule and thus enable us numerically to describe the character of each mode.

The isotropic chemical shifts are frequently used as an aid in identification of organic compounds and accurate predictions of molecular geometries are essential for reliable studies of magnetic properties. The B3LYP method allows calculating the shielding constants with accuracy and the GIAO method is one of the most common approaches for calculating nuclear magnetic shielding tensors. The ^{1}H and ^{13}C NMR isotropic shielding were calculated with the GIAO method [51,52] using the optimized parameters obtained from B3LYP/6-311++G(d,p) method.

In order to understand the electronic properties, such as HOMO–LUMO energies, dipole moment, absorption wavelengths, and oscillator strengths were calculated using B3LYP method of the TD-DFT [53–56] and 6-311++G(d,p) basis set, based on the optimized structure. Moreover, GaussSum 2.2 [57] was used to calculate group contributions of the molecular orbitals and to prepare TDOS or DOS, the PDOS and OPDOS spectra. The contribution of a group of a molecular orbital was calculated using Mulliken population analysis. The PDOS and OPDOS spectra were created by convoluting the molecular orbital information with Gaussian curves of unit height and a FWHM (Full Width at Half Maximum) of 0.3 eV.

The molecular electrostatic potential surface (MEPs) of the present molecule is illustrated and evaluated. The changes the heat capacity, entropy, and enthalpy of title molecule were investigated for the different temperatures (from 100 K to 700 K) from the vibrational frequency calculations in gas phase by using B3LYP/6-311++G(d,p) method. To calculate the NLO properties such dipole moment, mean polarizability and first static hyperpolarizability of the headline molecule the finite field approach DFT were used.

4. Results and discussion

4.1. Potential energy surface (PES) scan and conformational isomers

In this part of this study, as model system boronic acid and two fluorine atoms were chosen to investigate the possible conformers of the 3,5-DFPBA. In order to describe conformational flexibility of the title molecule, the energy profile as a function of C–C–B–O torsion angle was achieved with B3LYP/6-311G++(d,p) method (Fig. S1). Our calculations show that the 3,5-DFPBA molecule have three possible conformations, *cis–trans*, *trans–trans* and *cis–cis* (abbreviated as ct, tt and cc, respectively) for title molecule, do not differ greatly in energy, but demonstrate that conformation *ct* has the lowest energy, illustrated in Fig. 1, dependent on the positions of the hydrogen atoms bonded to oxygen, whether they are directed away from or toward the ring. From the calculations, the optimized structure of 3,5-DFPBA was calculated to exist in a planar structure for the *cc* forms (ca. 35.9°) while the other *ct* and *tt* forms of the molecule were calculated to a planar structure (ca. 180.0°) evident C–C–B–O torsional angle by using 6-311++G(d,p) basis set. The B–C rotational barrier in *tt* and *cc* forms was calculated to be ca. 2–3 kcal/mol (Fig. S1), which is significantly high as compared the B–C barrier *ct* form of molecule.

The energies of different conformation of the title molecule were optimized B3LYP/6-311++G(d,p) level of calculations. *ct* form is the more stable conformer than the other conformers. Three conformers of the 3,5-DFPBA molecule energies and energy difference [the relative energy of the other conformers was as: $\Delta E = E(Cn) - E(ct)$, the conformer ct is the lowest energy as reference point] are determined in Table 1. According to the DFT calculation of conformers with 6-311++G(d,p) basis set, the conformer *ct* is predicted more stable from 1.5652 kcal/mol to 3.4207 kcal/mol than the other conformers of the title molecule. The stability order for 3,5-DFPBA conformers is cis–trans > trans–trans > cis–cis form. Therefore, in the present work we have focused on cis–trans form of 3,5-DFPBA molecule to clarify molecular structure and assignment of vibrational spectra.

The geometric parameters (bond lengths and bond angles), vibrational frequencies, NMR chemical shifts and UV absorption

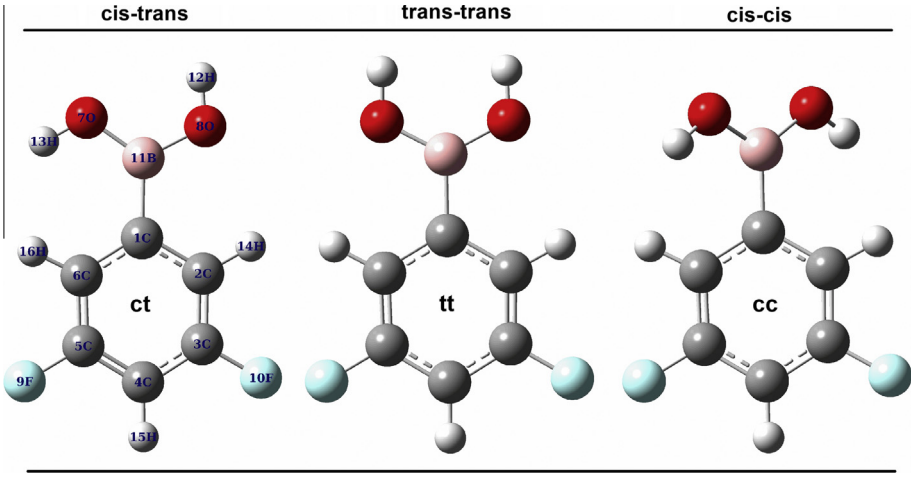

Fig. 1. The theoretical monomer structures of 3,5-DFPBA.

Table 1
Calculated energies and energies difference for three conformers of 3,5-DFPBA by DFT (B3LYP/6-311++G(d,p)) method.

Conformers	Energy		Energy differences[a]		Dipole moment
	(Hartree)	(kcal/mol)	(Hartree)	(kcal/mol)	(Debye)
Cis–Trans (ct)	−606.93171869	−380855.4193	0.0000	0.0000	1.898
Trans–Trans (tt)	−606.92922444	−380853.8542	0.0025	1.5652	4.326
Cis–Cis (cc)	−606.92626752	−380851.9987	0.0055	3.4207	1.302

[a] Energies of the other two conformers relative to the most stable *Cis–Trans* conformer.

of title molecule were reported by using 6-311++G(d,p) with the comparing experimental results in following sections.

4.2. Geometrical structures

The crystal structure of the phenylboronic acid and 2,4-difluorophenylboronic acid [12,21] (structurally similar molecules with our title molecule) were studied, however 3,5-DFPBA are not available in the literature until now. Therefore we compared geometric parameters with these molecules. The atomic numbering schemes of all conformers (ct, tt and cc) of the 3,5-DFPBA are shown in Fig. 1. Also the atomic numbering schemes of dimer *ct* form of the 3,5-DFPBA are shown in Fig. 2. The optimized geometry parameters of the molecule (monomeric and dimeric structure) are given in Table 2, comparing to the experimental values, in accordance with the atom numbering Fig. 1. The optimized geometry parameters of all conformers (*ct*, *tt*, *cc*) of the 3,5-DFPBA were given Table S1. From the data shown in tables, it is seen that the B3LYP level of theory is computed slightly bigger than experimental values of phenylboronic acids and 2,4-difluorophenylboronic acid. Taking into account that the molecular geometry of molecule in gas phase may be different from in the solid phase, owing to extended hydrogen bonding and stacking interactions there is reasonable agreement between the calculated and experimental geometric parameters.

The C–H bonds for the title molecule are approximately equal to for experimental values both of phenylboronic acid [12]. The similar behaviors are valid between the C–C ring bond lengths and angles the 3,5-DFPBA by using B3LYP/6-311++G(d,p) level of theory. We calculated the CC bond lengths in the ranges 1.384–1.404 Å for monomer and dimer structure of the ct form of the title molecule using by using B3LYP/6-311++G(d,p) level of theory in this study, showed well correlation in literature [12,21].

Typical B–O distances generally are ca. 1.360 Å [15] consistent with relatively strong π-interactions. However the few boronic acids including phenylboronic acid molecule, Chen et al. found approximately same value of this bond length by using HF/6-31G(d) levels of theory [11]. For the 3,5-dichlorophenylboronic

Table 2
Bond lengths (Å) and bond angles (°) experimental and optimized of 3,5-DFPBA for *ct* conformer.

Parameters	Experimental		B3LYP/6-311++G(d,p)	
	X-ray[a]	X-ray[b]	Monomer	Dimer
Bond lengths (Å)				
C1–C2	1.404 (3)	1.382 (3)	1.404	1.404
C1–C6	1.402 (3)	1.394 (3)	1.403	1.403
C1–B11	1.568 (3)	1.566 (3)	1.572	1.572
C2–C3	1.389 (3)	1.370 (3)	1.384	1.384
C3–C4	1.378 (5)	1.363 (4)	1.388	1.388
C3–F10	–	1.358 (3)	1.353	1.353
C4–C5	1.384 (5)	1.366 (4)	1.386	1.386
C5–C6	1.390 (4)	1.374 (3)	1.385	1.386
C5–F9	–	1.364 (3)	1.354	1.353
O7–B11	1.378 (2)	1.338 (3)	1.371	1.390
O7–H13	0.750 (5)	0.841 (15)	0.960	0.961
O8–B11	1.362 (2)	1.361 (3)	1.365	1.350
O8–H12	0.750 (5)	0.841 (15)	0.963	0.975
$C–H_{average}$	1.000 (5)		1.083	1.083
Bond angels (°)				
C2–C1–C6	117.2 (2)	114.6 (2)	118.7	118.7
C2–C1–B11	120.8 (2)	125.3 (2)	119.2	118.7
C6–C1–B11	122.0 (2)	120.1 (2)	122.1	122.7
C1–C2–C3	121.8 (2)	125.1 (2)	119.4	119.5
C1–C2–H14	120.0 (2)	118.5 (2)	120.8	120.6
C3–C2–H14	120.0 (2)	118.5 (2)	119.8	119.9
C2–C3–C4	119.5 (3)	116.4 (2)	122.9	122.9
C2–C3–F10	–	118.2 (2)	119.1	119.1
C4–C3–F10	–	116.7 (2)	118.0	118.0
C3–C4–C5	120.3 (2)	123.0 (2)	116.7	116.7
C3–C4–H15	120.0 (2)	–	121.7	121.7
C5–C4–H15	120.0 (2)	–	121.6	121.6
C4–C5–C6	120.1 (3)	117.9 (2)	122.7	122.7
C4–C5–F9	–	–	118.3	118.4
C6–C5–F9	–	–	119.0	119.0
C1–C6–C5	121.1 (2)	122.9 (2)	119.6	119.6
C1–C6–H16	120.0 (2)	–	122.5	122.7
C5–C6–H16	120.0 (2)	–	117.8	117.6
B11–O7–H13	111.0 (1)	116.0 (2)	115.6	115.2
B11–O8–H12	111.0 (1)	115.0 (2)	112.7	115.3
C1–B11–O7	125.0 (2)	123.8 (2)	124.4	122.5
C1–B11–O8	118.7 (2)	117.4 (2)	118.0	119.1
O7–B11–O8	116.3 (2)	118.7 (2)	117.6	118.4

[a,b] The X-ray data from Ref. [12,21].

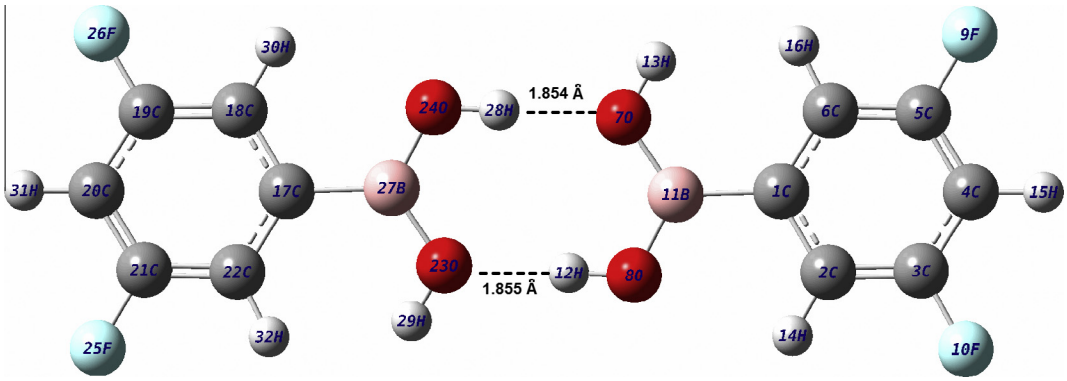

Fig. 2. The theoretical dimer structure of 3,5-DFPBA.

acid, this bond for different forms were found in the range of 1.364–1.372 Å [28], and also in the previous work, B–O distances including for different forms were calculated from 1.366 Å to 1.373 Å for 3,4-dichlorophenylboronic acid [26]. For the 2,4- and 2,6-dimethoxyphenylboronic acid molecule, B–O distances including ct (C_S and C_1 point group) form were found from 1.371 Å to 1.375 Å and including all different forms were found from 1.365 Å to 1.373 Å, respectively [29,30]. In our title molecule, the optimized B–O bond lengths obtained in the range 1.365 Å and 1.371 Å. These values showed more consistent with above mentioned the calculation results and experimental values [12,21]. However we also calculated these bands at 1.350 Å and 1.390 Å for the dimer structure of the molecule. This differences can be derived from inter and intra-molecular interaction.

The optimized B–C bond length of the 3,5-DFPBA was calculated at 1.572 Å (for monomer and dimer structures). The experimental values of phenylboronic acid and 2,4-difluorophenylboronic acid were observed 1.568 Å and 1.566 Å [12,21]. Bhat et al. [58] calculated B–C bond lengths at 1.566 Å and 1.567 Å in the lowest form for phenylboronic acid using B3LYP and MP2 methods, respectively. The C–B bond length is slightly greater than that typically found in boroxines, indicating a weakening of this bond by the electron-withdrawing nature of the C–F group [24].

The C–X (X; F, Cl, Br ...) bond length indicates a considerable increase when substituted in place of C–H. This bond length (fluorine atom) were observed [59] and calculated [60] for 2,3-difluorophenol molecule. The bond distance C–F is approximately similar experimental value 1.357 Å [61] which is in good agreement with calculated value in the previous study for 5-fluoro-salicylic acid [62]. Horton et al. the C_3–F_{10} and C_5–F_9 observed 1.342 Å and 1.343 Å in pentafluorophenylboronic acid [15], and Kurt [24] calculated these bonds 1.336 Å and 1.336 Å using B3LYP/6-311G(d,p) basis set. In this paper we obtained at 1.353 Å and 1.354 Å (C_3–F_{10} and C_5–F_9) respectively, showing good correlation. These bonds also show good agreement experimental values, observed values of 2,4-difluorophenylboronic acid [21]. The dimer C–F bonds are nearly the same for the monomer structure of the studied molecule.

The ring C–C–C bond angles calculated in the range of 116.7–122.9° showing well correlation with the experimental values and normal values (120.0°) of the six-membered phenyl ring. However the C_3–C_4–C_5 bond angle deviated from normal value, this may be due to attached fluorine atoms in phenyl group and this can distorted symmetries and normal values. All calculated bond angles showed the small difference from experimental values this can be due to calculation belongs to vapor phase and experimental result belong to solid phase.

Interestingly the geometry optimization performed on the title compound indicated that it exhibits intramolecular hydrogen bond interaction. Calculated short d(O–H···O) of the hydrogen bonds (1.854 Å) indicates strong hydrogen bonding between the monomeric units of 3,5-DFPBA. The O–H and B–O distances involved in the hydrogen bonds are lengthened upon dimerization, due to the redistribution of partial charges on the atoms involved. Similar effect was also obtained on the O–B–O and B–O–H angles. Most probably, the oxygen lone pairs have a resonance interaction with the empty p orbital of boron, which forces the hydrogen to be in the O–B–O plane. Two hydrogen atoms are in the O–B–O plane.

4.3. Vibrational spectral analysis

The vibrational frequencies were calculated C_S symmetry for ct and cc conformers and C_{2v} symmetry for tt conformer. Because of the imaginary frequency (−85 cm^{-1}), the calculation showed that the conformer *cc* is unstable conformer in C_S point group symmetry. Therefore, in order to obtain the stable structure, the *cc* form was converted to non-planar structure. However, according to Gaussian log files, *ct* and *tt* forms are C_S and C_{2v} symmetry group, because of obtained all positive frequencies.

The molecule of the 3,5-DFPBA consists of 16 atoms and it has 42 normal vibrational modes. On the basis of a C_S symmetry, the 42 fundamental vibrations of the *ct* form of the 3,5-DFPBA can be distributed as 29A + 13A. If we take the C_{2v} symmetry of the trans–trans (*tt*) form of this molecule into account, 42 normal vibrations can be distributed as $15A_1 + 5A_2 + 8B_1 + 14B_2$ but the *cc* form has C_1 symmetry cannot be distributed as stay 42A. In *ct* and *tt* form of the molecule, boronic acid and phenyl ring are in the same plane.

The recorded (FT-IR and FT-Raman) and calculated vibrational wavenumbers and assignments with TED are given in Table 3 for the most stable conformer (*ct*) (monomer and dimer structures) of studied molecule. All vibrations are active in both IR and Raman. Modes are numbered from smallest to biggest frequency within each fundamental wavenumbers, ν. The symmetry species of all the vibrations are given in the second column and in the last column is given a detailed description of the normal modes based on the TED.

In order to acquire the spectroscopic signature of the 3,5-DFPBA, we performed a wavenumber calculation analysis using DFT/B3LYP/6-311G++(d,p) basis set [46]. The calculations were made for free molecules in vacuum, while experiments were performed for solid sample, therefore there are disagreements between calculated and observed vibrational wavenumbers, and some frequencies are calculated, however these frequencies are not observed in the FT-IR and FT-Raman spectra. To the best of our knowledge there is no vibrational data for gas phase of the title molecule. Therefore we have to compare calculated results with those of solid phase vibrational spectrum of title molecule. The experimental and calculated infrared and Raman spectra were given in Figs. 3 and 4. The calculated IR and Raman spectra are shown in figures for comparative purpose, where the calculated intensity is plotted against harmonic vibrational wavenumbers.

The aim of this part of the study is the assignment of the vibrational absorptions to make a comparison with the related molecules and also with the results obtained from the theoretical calculations. There are some strong frequencies useful to characterize in the infrared and Raman spectra. It is worth mentioning that, for our molecule, the stretching vibrational modes are OH, CH, CC, CF, BO, CB and CCH, BOH, CCC, CCF, CBO, CCB in plane bending and torsion modes assigned out-of plane bending of C–H and O–H are the bending vibrational modes for title molecule. However, there is great mixing of the ring vibrational modes and also between the ring and substituent modes. The descriptions of the modes are very complex because of the low symmetry of the studied molecule. Especially, in plane modes and out of plane modes are the most difficult to assigned due to mixing with the ring modes and also with the substituent modes. Therefore, we discussed here only had strong frequencies of the calculated modes and had experimental values.

4.3.1. OH modes

The O–H stretching band is characterized by very broadband appearing near about 3400–3600 cm^{-1} and extremely sensitive to formation of hydrogen bonding. In the O–H region, very strong and broad bands in the spectra of some boronic acid molecules occur at ca. 3300 cm^{-1}. The assignment of these bands to O–H stretching vibrations is comprehensible. The strength and broadening wavenumbers of these bands suggest that intra-molecular hydrogen bonding occurs in different environments of boronic acids [22]. In the spectra of phenylboronic acid (3280 cm^{-1} in IR) [22], 2-fluorophenylboronic acid (3467 cm^{-1} in FT-IR) [23], pentafluorophenylboronic acid, (3467, 3410 cm^{-1} in FT-IR) [24],

Table 3
Comparison of the calculated harmonic frequencies and experimental (FT-IR and FT-Raman) wavenumbers (cm^{-1}) using by B3LYP method 6-311++G(d,p) basis set for monomer and dimer structures of ct form of 3,5-DFPBA.

Modes no	Sym. species	Theoretical/monomer		Theoretical/dimer		Experimental		TED[b] (⩾10%)
		Unscaled freq.	Scaled freq.[a]	Unscaled freq.	Scaled freq.[a]	FT-IR	FT-Raman	Monomer
ν1	A″	5	5	44, 23	43, 23		36	τCCBO(97)
ν2	A″	125	123	135, 132	133, 130		107	τCCCB(44), τCCBO(15), τCCBH(15)
ν3	A′	141	139	185, 183	182, 180		169	r[δCCB(66), δCBO(23)]
ν4	A″	231	227	232, 232	228, 228		195	γCF[τCCCF(55), τCFCH(10)], τCCCC(13)
ν5	A″	244	240	247, 247	243, 243		243	γCF[τCCCF(38), τCCCC(23)], τCFCH(13)
ν6	A′	286	282	308, 291	303, 286		267	δCCF(40), νCB(17), δCBO(14)
ν7	A′	356	350	372, 362	366, 356		342	δCCF(41), δBO_2 (14), νCC(10)
ν8	A′	358	352	384, 363	378, 357			δCBO(54), δCCF(17)
ν9	A″	446	439	438, 430	430, 422	440		τCBOH(47), τBOOH(33)
ν10	A″	468	460	494, 493	485, 485	465		γOH[τBOOH(16), τCBOH(26)], τCCBO(14), τCCCC(14)
ν11	A′	514	505	514, 514	505, 505	502	503	δCCC(43), δCCF(31)
ν12	A′	517	508	531, 524	522, 515			δCCC(33), δBO_2(15), δCBO(10), νCF(10)
ν13	A′	551	541	554, 553	545, 544	534	536	δCCF(48), δCCB(14), δCBO(13)
ν14	A′	563	554	612, 576	602, 566			νCF(18), δBOO(15), νCC(14), νCB(11)
ν15	A″	580	571	790, 742	777, 730			γOH[τBOOH(42), τCBOH(31)]
ν16	A″	605	595	606, 606	595, 595	616	595	τCCCH(18), τCCCC(17), τCCCF(16), τCFCH(16)
ν17	A″	663	652	659, 658	647, 647	663	651	τCCCC(37), τCCCH(27), γOH[τBOOH(16)]
ν18	A″	715	703	714, 713	702, 701	730	700	γCH[τCCBO(35), τCCCH(13)], τCBOH(11), τBOOH(10)
ν19	A″	856	841	857, 857	843, 843		806	γCH[τCFCH(27), τCCCH(26)], τCCBH(14)
ν20	A″	872	857	873, 873	858, 858	862		γCH[τCCCH(55), τCFCH(30)]
ν21	A′	890	875	888, 888	873, 872	881		νBO(24), νCB(18), νCF(16), δCCH(13), νCC(13)
ν22	A″	913	898	914, 914	899, 899	905		γCH[τCCCH(32), τCFCH(28), τCBCH(24)]
ν23	A′	986	969	1027, 1013	1009, 995			δOH [δBOH(59)], νBO(10)
ν24	A′	1000	983	995, 994	978, 978	980		νCF(28), νCC(25), δBOH(13)
ν25	A′	1018	1001	1019, 1016	1002, 999			νCC(42), δCCC(36)
ν26	A′	1026	1008	1189, 1089	1169, 1071		1007	δOH[δBOH(79)], νBO(17)
ν27	A′	1127	1108	1152, 1126	1132, 1107		1099	δCCH(46), νCC(20), νCF(11)
ν28	A′	1133	1114	1134, 1132	1115, 1112	1117	1115	δCCH(50), νCF(30)
ν29	A′	1255	1234	1255, 1255	1234, 1233	1233	1234	δCCH(68), νCC(22)
ν30	A′	1280	1258	1291, 1281	1269, 1259			νCF(38), νBO(12)
ν31	A′	1340	1317	1341, 1335	1318, 1312	1326		νCC(70), δCCH(24)
ν32	A′	1373	1349	1364, 1349	1341, 1326		1337	νBO(25), νCB(24), νCF(10), δBOH(10)
ν33	A′	1389	1365	1421, 1419	1397, 1395	1378	1365	νBO(64), νCC(13)
ν34	A′	1459	1434	1465, 1458	1440, 1433	1432		δCCH(18), νBO(12)
ν35	A′	1501	1475	1502, 1502	1477, 1477	1474	1475	νCC(40), δCCH(27)
ν36	A′	1624	1597	1624, 1624	1597, 1596	1587		νCC(67), δCCH(13)
ν37	A′	1654	1626	1654, 1654	1626, 1626	1639	1625	νCC(73)
						1771		Overtone + combination
						2359		Overtone + combination
ν38	A′	3175	3041	3170, 3170	3037, 3037			νCH(100) (C_6–H_{16})
ν39	A′	3211	3076	3211, 3211	3076, 3076	3063	3067	νCH(100) (C_2–H_{14})
ν40	A′	3219	3083	3219, 3219	3083, 3083	3092	3092	νCH(100) (C_4–H_{15})
ν41	A′	3848	3686	3624, 3594	3472, 3443			νOH(100) (O_8–H_{12})
ν42	A′	3888	3725	3875, 3875	3712, 3712			νOH(100) (O_7–H_{13})

[a] Wavenumbers in the ranges from 4000 to 1700 cm^{-1} and lower than 1700 cm^{-1} are scaled with 0.958 and 0.983 for B3LYP/6-311++G(d,p) basis set, respectively.
[b] ν; stretching, γ; out-of plane bending, δ; in-plane-bending, τ; torsion, ρ; scissoring, ϕ; twisting, Γ; rocking.

4-chloro and 4-bromophenylboronic acid (3276, 3249 cm^{-1} and 3276, 3164 cm^{-1} in FT-IR) and (3175, 3106 and 3108 cm^{-1} in FT-Raman) [25], 3,4-dichlorophenylboronic acid (3465, 3425 cm^{-1} in FT-IR) [26], 3,5-dichlorophenylboronic acid (3443, 3397 cm^{-1} in FT-IR and 3480, 3440 cm^{-1} in FT-Raman) [28]. Also we recorded this band at 3400 and 3332 cm^{-1} in FT-IR spectrum and predicted value of 3685 (O_7–H_{11}) and 3692 cm^{-1} (O_8–H_{10}) in the previous study for the structurally similar compound 2,3-diflourophenyl boronic acid molecule [31]. In this study, these bands are not observed both FT-IR and FT-Raman spectra, but computed (ν41 and ν42) at 3686 (O_8–H_{12}) and 3725 cm^{-1} (O_7–H_{13}) that show agreement with the literatures for structurally similar molecules [23–26,28]. As expected this mode is pure stretching mode as it is evident from TED column, it is almost contributing 100%. As discussed in literature [23–26,28], with halogen (F, Cl, Br, ...) substitution, O–H stretching vibrations shift to a higher wavenumber region [63]. This means that, in the boronic acid part, O–H vibrations are sensitive due to halogen coordination. Also there is downshift calculated at 3472, 3443 cm^{-1} (O_8–H_{12}) and 3712, 3712 cm^{-1} (O_7–H_{13}) for O–H stretching vibration in dimer structure, it can be due to the presence of intermolecular interaction.

The O–H in-plane bending vibrations, in general lies in the region 1150–1250 cm^{-1} and is not much affected due to hydrogen bonding unlike to stretching and out-of-plane bending frequencies [64]. The modes ν23, ν24, ν26 and ν32 assigned as OH in-plane bending modes predicted at 969, 983, 1008 and 1349 cm^{-1} and out-of-plane bending vibrations computed at 439, 460, 571, 652 and 703 cm^{-1} in this paper for 3,5-DFPBA. This band at 1007 and 1337 cm^{-1} in FT-Raman and at 980 cm^{-1} in FT-IR is assigned (in-plane) while OH out-of-plane bending vibration is assigned at, 440, 465, 663 and 730 in FT-IR cm^{-1} 651 and 700 cm^{-1} in FT-Raman, respectively. The in-plane-bending vibration δO–H is observed in the range 1100–960 cm^{-1} in case of acenaphthene-5-boronic acid [32]. This band was observed at 1002 cm^{-1} for 2,3-difluorophenylboronic acid and at 1005 cm^{-1} for 3,4-dichlorphenylboronic acid . Theoretical value of OH out-of-plane bending and in-plane bending vi[26,31]bration are good coherent in experimental values and in literature [23–25,28–30]. The O–H

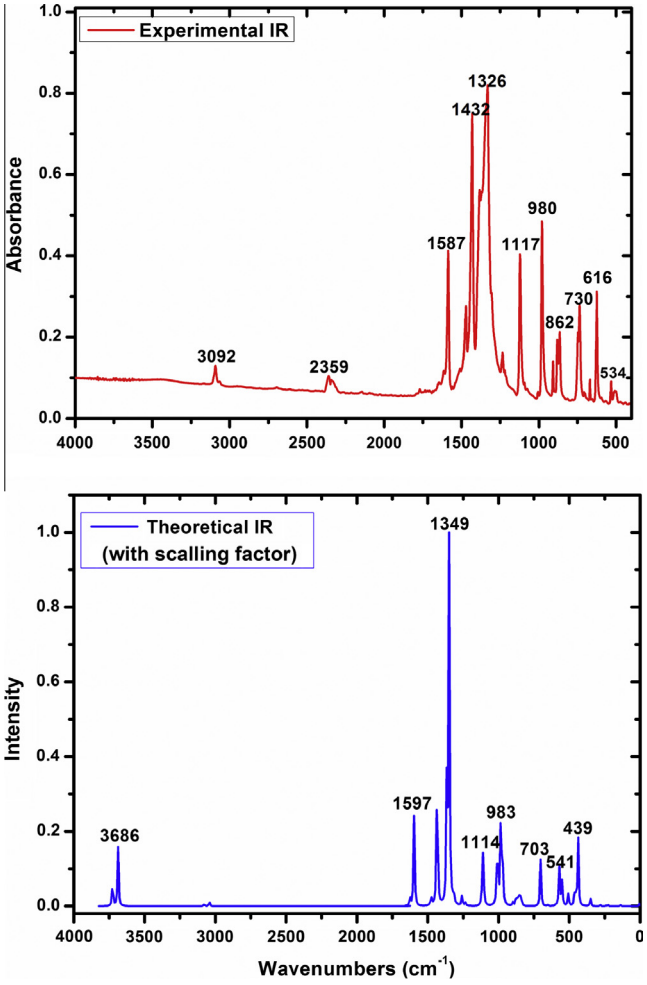

Fig. 3. The experimental and calculated infrared spectra of 3,5-DFPBA.

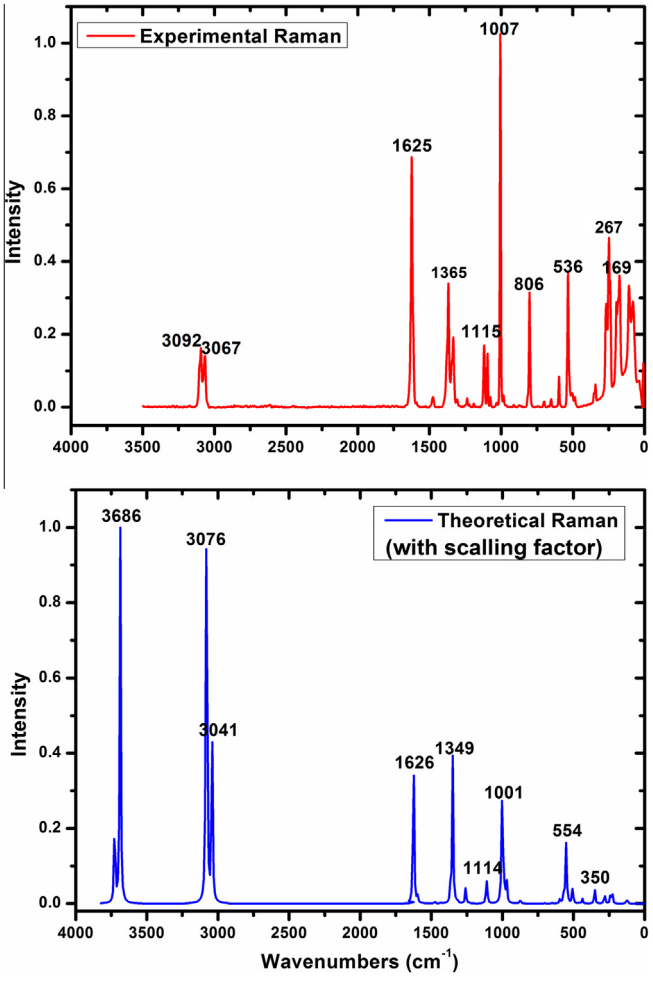

Fig. 4. The experimental and calculated Raman spectra of 3,5-DFPBA.

in plane bending and out of plane bending vibrations values in dimer conformations are increased, because of the hydrogen bonding effect through the $B(OH)_2$ groups (Table 3).

4.3.2. C–H modes

The substituted benzene like molecules give rise to C–H stretching, C–H in-plane and C–H out-of-plane bending vibrations. The hetero aromatic structure shows the presence of C–H stretching vibrations in the region 3000–3100 cm^{-1} which is the characteristic region for ready identification of C–H stretching vibration [65]. For the structurally similar compound 2,3-diflourophenyl boronic acid molecule the C–H stretch computed in the range of 3048–3070 cm^{-1} by the B3LYP/6-311++G(d,p) method and observed at 3048 and 3070 broad bands in FT-IR and with the recorded FT-Raman at 3040–3077 cm^{-1}, respectively [31]. These modes also discussed in literature, [23–28] these bands were predicted range of 3048–3070 cm^{-1} for structurally similar compounds. The aromatic C–H stretching of 3,5-DFPBA gives bands at 3063 and 3092 cm^{-1} in the FT-IR spectrum and at 3067 and 3092 cm^{-1} in the FT-Raman spectrum, computed in the range of 3041–3083 cm^{-1} for monomer and in the range of 3037–3083 cm^{-1} for dimer structure of *ct* form. As indicated by the TED, these three modes (ν38–40) involve approximately 100% contribution suggesting that they are pure stretching modes in this work; correspond to the stretching modes of C_2–H_{14}, C_4–H_{15} and C_6–H_{16} units. The aromatic C–H stretching bands are found to be weak, and this is due to a decrease in the dipole moment caused by reduction of negative charge on the carbon atom.

The C–H in-plane bending frequencies appear in the range of 1000–1300 cm^{-1} and C–H out-of-plane bending vibration in the range 750–1000 cm^{-1} for aromatic compounds [65,66]. For present molecule, the both in-plane and out-of plane C–H bending vibrations are observed in the region mentioned above (Table 3) and predicted values are coinciding very well with the observed frequencies. The C–H in-plane bending vibrations were observed at 1117, 1233, 1326, 1474, 1587 cm^{-1} in FT-IR and at 1099, 1115, 1234 and 1475 cm^{-1} in FT-Raman, are calculated at 1317 cm^{-1} and also in range of 1108–1234 cm^{-1} and 1434–1597 cm^{-1}, respectively. The C–H out of plane bending modes are assigned ν_{18-20} and ν_{22}, predicted in the range of 703–857 cm^{-1} and 898 cm^{-1}, respectively. These modes were observed at 730, 862, 905 cm^{-1} and 700, 806 cm^{-1} in FT-IR and FT-Raman, respectively. The TED contributions of in-plane and out-of plane modes indicate out-of plane modes are also highly pure. However the in-plane bending vibrations are contaminated other modes. All results for the above conclusions are in well agreement for the literature of the similar molecules [23–28]. If we take into account the dimer structure, the computed results are nearly the same and good correlation.

4.3.3. CC modes

The ring carbon–carbon stretching vibrations occur in the region 1430–1625 cm^{-1}. In general, the bands are of variable intensity and are observed at 1625–1590, 1575–1590, 1470–1540,

1430–1465 and 1280–1380 cm^{-1} from the frequency ranges given by Varsanyi [67] for the five bands in the region. The ring stretching vibrations are very much important and highly characteristic of the aromatic ring itself. In the aromatic C–C stretching region falls in the range of 1620–1320 cm^{-1} the assignments of five bands in the IR spectra of phenylboronic acids [22]. Similarly, the C–C stretching modes were record for 2-fluorophenylboronic acid 1617–1034 cm^{-1} (IR) [23], 4-chlorophenylboronic acid 1596–1060 cm^{-1} and 1588–1085 cm^{-1} in the FT-IR and FT-Raman and 4-bromophenylboronic acid in the range of 1590–1010 cm^{-1} and 1588–1004 cm^{-1} in FT-IR and FT-Raman [25], 3,4-dichlorophenylboronic acid at 1591–1028 cm^{-1} in FT-IR and 1590–1035 cm^{-1} in FT-Raman [26], 3,5-dichlorophenylboronic acid in the range of 1570–969 cm^{-1} in FT-IR and 1584–995 cm^{-1} in FT-Raman [28], respectively. The C–C stretching vibrations were computed 1629–1465, 1304–1213, 1149–1063, 899, and 635 cm^{-1} by using B3LYP method and observed at 1628, 1266, 1214, 1154 cm^{-1} and 1626, 1590, 1474, 1292, 1269, 1215, 1148, 1065 cm^{-1} in FT-IR and FT-Raman, respectively for 2,3-difluorophenyl boronic acid molecule [31]. In the present work, C–C stretching vibrations were computed at 554, 875, 983, 1001, 1108, 1234, 1317, 1365, 1475, 1597 and 1626 cm^{-1} by B3LYP method for 3,5-DFPBA. The experimental values are in very good coherent, observed at 881, 980, 1233, 1326, 1378, 1474, 1587 and 1639 cm^{-1} in FT-IR, 1099, 1234, 1365, 1475 and 1625 cm^{-1} in FT-Raman, respectively. The main C–C stretching vibrations are calculated at 1317 and 1626 cm^{-1} with the TED contribution 70% and 73%. The C–C stretching vibrations generally showed pure modes according to their TED and some of these modes are contaminated other vibrations. The dimer structure also showed good coherent for experimental values especially for the up to the 1000 cm^{-1}.

The ring deformation, torsion and CCC bending modes are mixed with other modes. The calculated wavenumbers of these modes almost coincide with experimental data after scaling. The ring deformation, torsion and out-of-plane CCC bending modes are obtained in a large region like vibrational modes of the studied molecule. Therefore, these modes will not be discussed here. Also the TEDs of these vibrations are not pure modes as it is evident from the last column of Table 3.

4.3.4. C–F modes

In the fluorine compounds, very intense absorption occurs in the region 1100–1350 cm^{-1} [63,68]. Mono-fluorinated compounds have a strong band between 1000 and 1110 cm^{-1}; with more than one fluorine atoms, the band splits into two bands, one for the symmetric mode and one for the asymmetric mode [69]. Infrared spectra of a number of mono- and di-substituted fluorine derivatives have been studied by Narasimham et al. [70] and those of tri- and tetrafluorobenzene by Ferguson et al. [71]. They have assigned the frequency 1250 cm^{-1} to C–F stretching mode of vibration. In analogy to these assignments, infrared frequency observed at 1235 cm^{-1}, which is strong in intensity, is assigned as C–F stretching frequency for 1-fluoro-2,4-dinitrobenzene [72], corresponding Raman frequency for the same mode is 1246 cm^{-1}. The FT-IR peaks observed at 1279, 1238 cm^{-1}, FT-Raman peaks at 1283, 1238 cm^{-1} and at 1277, 1250 cm^{-1} (FT-IR), 1275, 1249 cm^{-1} (FT-Raman) are due to the C–F stretching of 2,3- and 2,4-diflouroboronic acid, respectively [69]. For 2,3-difluorophenol, Sundaraganesan et al. [60] assigned the strong bands at 1331 and 1279 cm^{-1} in FT-IR spectrum due to C–F stretching mode, and their counterpart in Raman spectrum is at 1332 and 1280 cm^{-1}. In previous study, we have assigned the strong bands at 1254 and 1222 cm^{-1} in the FT-IR spectrum due to the C–F stretching mode. Their counterpart in the Raman spectrum is at 1274 and 1245 cm^{-1} [62]. The CF stretching modes were calculated 1264–1070 and 899, 635 cm^{-1} by using B3LYP method and observed at 1269, 1215 and 1178 cm^{-1} in FT-Raman spectrum and 1266, 1214, 1183 and 648 cm^{-1} in FT-IR spectrum [31]. From Table 3, it can be shown that TED calculations give some ring C–F stretching contaminated with other modes. We were computed at 1349, 1258, 1114, 1108, 983, 875, 554 and 508 cm^{-1} for CF stretching modes, showed in well correlation with the experimental values. The observed values are listed at 1117, 980 and 881 cm^{-1} in FT-IR spectrum and 1337, 1115 and 1099 cm^{-1} FT-Raman spectrum for the 3,5-DFPBA molecule.

In-plane bending and out-of-plane bending modes of C–F vibrations appear in variable region according to molecular structure and state of the fluorine substituent. The C–F in-plane bending frequency appears in the region 350–250 cm^{-1} [73]. The band at 304 cm^{-1} in FT-Raman is assigned to C–F in-plane bending. The theoretically calculated value at 298 cm^{-1} (unscaled 303 cm^{-1}) exactly correlates with experimental observations for 2,3-diflouroboronic acid [39]. The C–F in-plane bending wavenumbers were computed by B3LYP method in the region 380–255 cm^{-1} for pentaflourophenylboronic acid [24]. The band at 292 cm^{-1} in FT-Raman was assigned to C–F in-plane bending mode for 2,3-difluorophenol [55]. Sundaraganesan et al. [74] observed strong band at 759 cm^{-1} in FT-IR and very strong band at 750 cm^{-1} in FT-Raman was assigned to C–F in-plane bending mode for 2-amino-4,5-difluorobenzoic acid molecule. In present work, we have assigned at 282, 350, 352, 505, 541 cm^{-1} for C–F in plane bending vibrations. We also identified according to TED as a major contribution mode 13 for in plane modes.

The C–F out-of-plane bending mode has been identified as the frequency 590 cm^{-1} as a weak band in FT-IR and 592 cm^{-1} in FT-Raman [74]. For 2-fluorophenylboronic acid molecule, Erdogdu et al. [23] observed one band at 520 cm^{-1} both in the FT-IR and in the FT-Raman spectra. The C–F out-of-plane bending modes of the bands are supported in literature [75–77]. In present work we have assigned at 227 and 240 cm^{-1} (monomer) 228 and 243 cm^{-1} (dimer) for out-of plane bending modes. The values for in plane out-of-plane bending mode (both monomer and dimer) are supported in very good agreement with the experimental results (see Table 3).

4.3.5. B–O modes

The compounds containing B–O linkage, such as boronate and boronic acid are characterized by strong B–O stretching mode at 1380–1310 cm^{-1} [78]. The B–O asymmetric stretching band of the phenylboronic acid occurs at 1370 cm^{-1} in the infrared spectrum [22] and at 1375 cm^{-1} for the phenylboronic acid linkage [79]. The νB–O stretching vibrations were observed at 1352 and 1351, 1389 cm^{-1} in FT-IR and in FT-Raman and calculated at 1345, 1371 and 1002 cm^{-1} for derivatives of the phenyl boronic acid (2,3-DFPBA) molecule by using B3LYP method assigned as two symmetric and asymmetric modes by Karabacak et al. [31]. These bands are very intense and should also include the asymmetric stretching vibrations which are located at 1349 and 1350 cm^{-1} for phenylboronic, and pentafluorophenylboronic acids, respectively [22,24]. This band also was observed at 1385 cm^{-1} in the FT-IR and at 1370 cm^{-1} in the FT-Raman spectra for 2-fluorophenylboronic acid [23]. The corresponding bands were observed at 1392 cm^{-1} as very strong bands in FT-IR and at 1409 cm^{-1} as weak bands in FT-Raman spectra [28]. The other strong band in the spectrum observed at 1379 cm^{-1} [26]. The band is very intense and should include also the ν(B–O) asymmetric stretching vibration. Kurt [25] observed the νB–O stretching vibration at 1373 and 1361 cm^{-1} for 4-chlorophenylboronic acid and 4-bromophemylboronic acid, respectively. The B–O asymmetric/symmetric stretching bands with dominant TED were calculated at 1354 and 1308 cm^{-1} and were assigned with strong FT-IR peaks

at 1345/1314 cm^{-1} and weak FT-Raman peaks at 1349/1321 cm^{-1} for acenaphthene-5-boronic acid [32]. In this study for the 3,5-DFPBA derivative of the phenyl boronic acid, νB–O stretching vibrations were observed at 881, 1378 and 1432 cm^{-1} in FT-IR and 1007, 1337 and 1365 cm^{-1} in FT-Raman. We calculated at 875, 969, 1008, 1258, and in the range of 1349–1434 cm^{-1} by using B3LYP method assigned as two symmetric and asymmetric modes. The TED calculations show that the B–O stretching mode is nearly a pure mode in Table 3. We can also say when two fluorine atoms are substituted phenylboronic acid, the B–O vibration shifts to higher wavenumbers in the FT-IR spectrum and FT-Raman spectrum, respectively. Also there are differences between the monomer and dimer structure these can be the presence of intermolecular interaction.

The in-plane bending BO_2 mode has been observed as a doublet at 502 cm^{-1} for 2,3-difluorophenylboronic acid [31], the mode is observed at higher wavenumber for phenylboronic acids and dichlorphenylboronic acid [26,31]. The in-plane BO_2 were assigned at 485 cm^{-1} with 35% TED contribution for acenaphthene-5-boronic acid [32]. In our paper the in-plane δBO_2 modes were calculated at 350 (observed at 342 cm^{-1} FT-Raman) and 508 cm^{-1} for the present molecule.

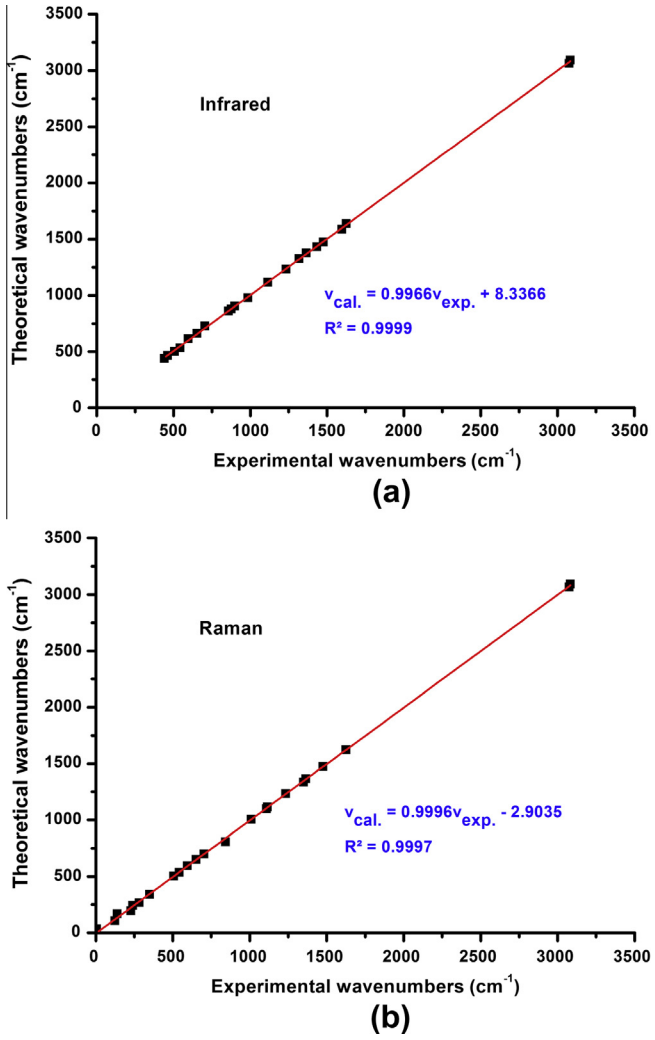

Fig. 5. The correlation graphics of experimental and calculated wavenumbers of 3,5-DFPBA.

The CBO in-plane bending vibrations were also predicted (282, 352, 508 and 541 cm^{-1} by using B3LYP method) and compared with the experimental findings as 267 and 536 cm^{-1} in FT-Raman and 534 cm^{-1} in FT-IR. The modes δCBO were computed at 312, 353 and 513 cm^{-1} and observed at 310, 350 and 501 cm^{-1} in FT-Raman and 502 cm^{-1} in FT-IR for 2,3-difluorophenylboronic acid [31]. Also Rani et al. computed at 352 and 459 cm^{-1} by using HF method and also observed at 145 and 430 cm^{-1} FT-Raman and FT-IR spectra, respectively for methyl boronic acid [33].

4.3.6. C–B modes

The mode of C–B stretching modes evaluate and the characteristic for boronic acids and its derivatives [17,22,23,28,31–34]. The C–B stretching modes of the arylboronic acid were observed at 1080 and 1110 cm^{-1} by Santucci and Gilman [80]. Faniran and Shurvell [22] also assigned the band at 1089 and 1085 cm^{-1} in the spectra of the normal and deuterated phenylboronic acids, respectively, and at 1084 cm^{-1} in diphenyl phenylboronate to the C–B stretching modes. Erdogdu et al. [23] were observed at 1354 and 708 cm^{-1} in FT-IR and at 701 cm^{-1} in FT-Raman for 2-flourophenylboronic acid and computed using B3LYP/6-311++G(d,p) and shifted by 265 cm^{-1} for the fluorine substitution. The C–B stretching band of 3,5-dichlorophenylboronic molecule was observed at 802 cm^{-1} as medium band in FT-IR and negatively shifted by ca. 280 cm^{-1} for the chlorine substitution [28]. These means those in the boronic acid part C–B vibrations are sensitive because of chlorine or fluorine substitution [23,28]. For n-butylboronic acid, these vibrations are assigned at 1147 and 1109 cm^{-1} by Cyrański et al. [34]. The calculated C–B stretching modes were computed at 1345, 899, 635 cm^{-1} for 2,3-difluorophenylboronic acid, observed at 1352 and 1351 cm^{-1} as the bands in FT-IR and FT-Raman, respectively, in well agreement [31]. The C–B stretching vibrations were observed at 881 and 267, 1337 cm^{-1} as the bands in FT-IR and FT-Raman, respectively and also shifted due to the fluorine substitution. The predicted C–B stretching values were computed at 282, 554, 875, 1349 cm^{-1} in well agreement in their experimental values and literature [17,22,23,28,31–34].

4.3.7. Analysis of vibrational calculations

The correlation graphics between the experimental and calculated wavenumbers were graphed, calculated by DFT/B3LYP method. The correlation graphics which described harmony between the calculated and experimental wavenumbers (Infrared and Raman) were given in Fig. 5a and 5b. As can be seen from Fig. 5, experimental fundamentals have a better correlation and the relations between the calculated and experimental wavenumbers are

Table 4
Experimental and theoretical, ^1H and ^{13}C NMR isotropic chemical shifts (with respect to TMS) of monomer and dimer structures of 3,5-DFPBA with DFT (B3LYP/6-311++G(d,p)) method.

Atoms	Carbon/B3LYP		
	Exp.	Monomer	Dimer
C(1)	116.66	139.02	139.00
C(2)	115.86	121.99	122.31
C(3)	164.31	171.89	171.64
C(4)	105.28	110.97	111.01
C(5)	161.03	171.95	171.72
C(6)	115.86	119.58	119.20
Atoms	Hydrogen/B3LYP		
	Exp.	Monomer	Dimer
H(12)	–	4.30	6.77
H(13)	–	4.92	5.24
H(14)	7.44	7.66	7.77
H(15)	7.22	7.12	7.06
H(16)	7.44	7.18	7.17

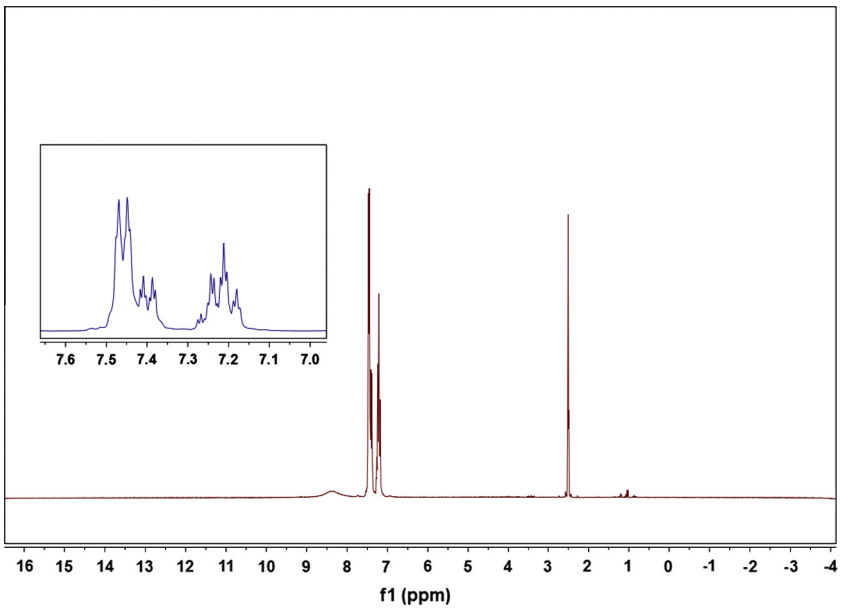

Fig. 6. ^{1}H NMR spectrum of 3,5-DFPBA in DMSO solution.

usually linear and described for infrared and Raman, respectively by the following equations:

$$\upsilon_{cal} = 0.9966\,\upsilon_{exp} + 8.3366 \quad (R^2 = 0.9999 \text{ for Infared})$$

$$\upsilon_{cal} = 0.9996\,\upsilon_{exp} - 2.9035 \quad (R^2 = 0.9997 \text{ for Raman})$$

4.4. NMR spectra

In order to explain the experimental observations of nuclear magnetic resonance, or NMR as it is abbreviated, of the molecule the quantum chemistry DFT calculations was performed and these values are evaluated. The first step; the full geometry optimization of the studied molecule was performed at second step; the gradient corrected DFT using the hybrid B3LYP method based on Becke's three parameters functional of DFT and GIAO method [51,52]. In NMR experiment, we are not directly interested in absolute shielding values but rather in chemical shift parameters with regard to a reference. ^{1}H and ^{13}C chemical shift calculations of the compound was made by the same method using 6-311++G(d,p) basis set IEFPCM/DMSO solution. Because of the accurate predictions of molecular geometries are essential for reliable calculations of magnetic properties. The isotropic shielding values were used to calculate the isotropic chemical shifts δ with respect to TMS $\delta_{iso}^{X} = \sigma_{iso}^{TMS} - \sigma_{iso}^{X}$.

The recorded and calculated (monomer and dimer) ^{1}H and ^{13}C chemical shifts in DMSO solution solvent are collected in Table 4. The atom statues were numbered according to Fig. 1. The experimental ^{1}H and ^{13}C NMR spectra of the 3,5-DFPBA are shown in Figs. 6 and 7, respectively. Generally, the proton chemical shift of organic molecules varies greatly with the electronic environment

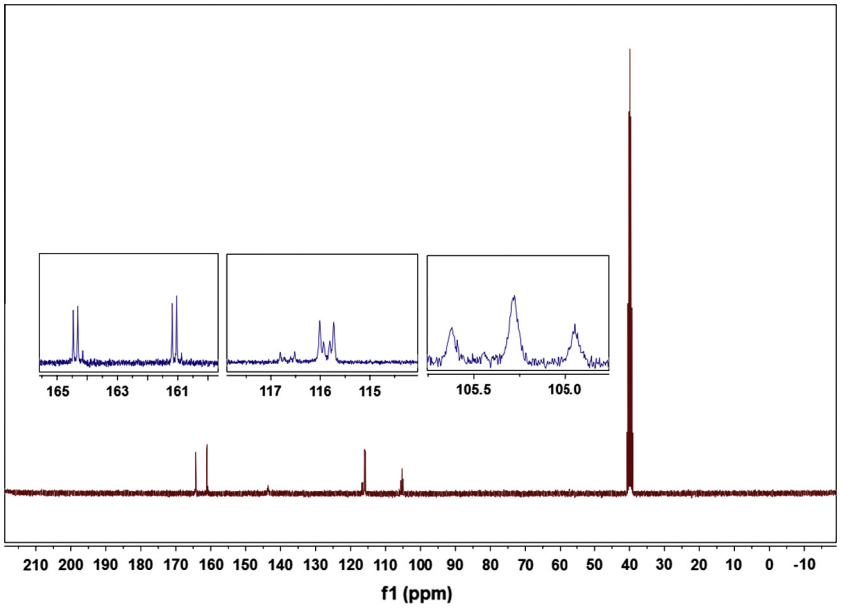

Fig. 7. ^{13}C NMR spectra of 3,5-DFPBA in DMSO solution.

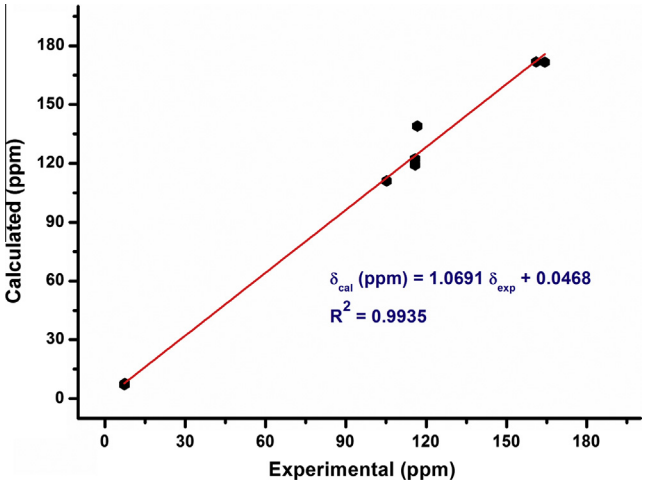

Fig. 8. The correlation graphics of experimental and calculated chemical shifts of 3,5-DFPBA.

of the proton. Some comments are concerning the presence or lack of electronic structure of molecule. Hydrogen attached or nearby electron-withdrawing atom or group can decrease the shielding and move the resonance of attached proton towards to a higher frequency, whereas electron-donating atom or group increases the shielding and moves the resonance towards to a lower frequency [81]. The chemical shifts of aromatic protons of organic molecules are usually observed in the range of 7.00–8.00 ppm. There is three signals of proton (^{1}H) of the molecule were calculated theoretically at 7.12–7.66 ppm (monomer) and 7.06–7.77 ppm (dimer), observed at 7.22–7.44 ppm experimentally for the aromatic proton of ring. The H_{12} value was computed smaller than H_{13} chemical shifts it can be due to the electronic environment of the H_{13} atom (the electronic charge density around of H_{13}) for monomer structure but H_{13} chemical shifts is smaller than H_{12} value for the dimer structure due to change the electronic structure for presence of the intermolecular effect. However the chemical shifts of these hydrogen atoms were not observed this may be due to the fluorine atoms and/or DMSO solvent effects. The deviation between experimental and computed chemical shifts of these protons may be due to the presence of intermolecular hydrogen bonding and the effect of solvent.

The region for the chemical shift values from 100 to 150 ppm are characteristic aromatic carbons, given signals in overlapped area [82,83]. The studied molecule is possessed of six carbon atoms, which is consistent with the structure on basis of molecular symmetry. Considering ^{13}C NMR the chemical shifts C_3 and C_5 are observed and calculated greater than other chemical shifts of carbon atoms. This increments can be due to the fluorine atom, attached these carbons. Namely, the fluorine atoms that electronegative substituent polarizes the electron distribution in its bond to carbon, therefore, the chemical shifts value of C_3 and C_5 bonded to fluorine atoms show calculated ^{13}C chemical shifts that is too high. The chemical shifts of these carbons were observed at 164.31 and 161.03 ppm while which was calculated 171.89 and 171.95 ppm, respectively. ^{13}C NMR chemical shifts of C_1, C_2, and C_6 atoms are nearly same magnitude this can be symmetry of electronic and magnetic structure of the molecule. Moreover, DMSO contains electronegative atoms such as oxygen and sulfur. Thus in our title molecule was affected this solution. Besides, due to shielding effect which the non-electronegative property of fluorine atoms, the chemical shift value of C_4 atom is lower than the others carbon peak. The ^{13}C NMR chemical shifts in the ring for the title molecule (except C_3 and C_5) are from 100 to 150 ppm both experimentally and theoretically showing good correlation with each other (Table 4).

Based on the ^{1}H and ^{13}C chemical shifts data collected (monomer and dimer structure) in Table 4 one can deduce that qualita-

Table 5
Experimental and calculated wavelengths λ (nm), excitation energies (eV), oscillator strengths (f) of monomer and dimer structures of 3,5-DFPBA in ethanol, water solution and gas phase.

λ (nm)	E (eV)	f	Assignments	Major contributes	λ (nm)	E (eV)
Monomer						
TD-DFT/ B3LYP/6-311++G(d,p) (ethanol)					Exp. (ethanol)	
251.23	4.93566	0.0382	$\pi-\pi^*$	H → L (83%), H − 1 → L + 1 (17%)	269.51	4.60094
219.96	5.63736	0.1625	$\pi-\pi^*$	H − 1 → L (84%), H → L + 1 (15%)	217.77	5.69408
199.19	6.22514	0.0002	$\pi-\pi^*$	H → L + 2 (96%)		
TD-DFT//B3LYP/6-311++G(d,p) (water)					Exp. (water)	
251.12	4.93796	0.0374	$\pi-\pi^*$	H → L (83%), H − 1 → L + 1 (17%)	269.85	4.59515
219.82	5.64086	0.1593	$\pi-\pi^*$	H − 1 → L (84%), H → L + 1 (15%)	215.84	5.74500
198.92	6.23354	0.0001	$\pi-\pi^*$	H → L + 2 (95%)		
TD-DFT//B3LYP/6-311++G(d,p) (gas phase)						
252.05	4.91966	0.0299	$\pi-\pi^*$	H → L (82%), H − 1 → L + 1 (17%)		
208.04	5.96040	0.0008	$\pi-\pi^*$	H → L + 2 (98%)		
195.99	6.32685	0.0009	$\pi-\pi^*$	H − 1 → L + 2 (98%)		
Dimer						
TD-DFT/ B3LYP/6-311++G(d,p) (ethanol)					Exp. (ethanol)	
251.61	4.92826	0.0	$\pi-\pi^*$	H → L (45%), H − 1 → L + 1 (38%)	269.51	4.60094
251.55	4.92946	0.0753	$\pi-\pi^*$	H − 1 → L (45%), H → L + 1 (38%)		
230.51	5.37942	0.0	$\pi-\pi^*$	H → L + 1 (46%), H − 1 → L (40%)	217.77	5.69408
TD-DFT//B3LYP/6-311++G(d,p) (water)					Exp.(water)	
251.48	4.93086	0.0001	$\pi-\pi^*$	H → L (45%), H − 1 → L + 1 (38%)	269.85	4.59515
251.42	4.93206	0.0735	$\pi-\pi^*$	H − 1 → L (45%), H → L + 1 (38%)		
230.41	5.38172	0	$\pi-\pi^*$	H − 1 → L (37%), H − 1 → L + 1 (14%)	215.84	5.74500
TD-DFT//B3LYP/6-311++G(d,p) (gas phase)						
252.60	4.90896	0.0001	$\pi-\pi^*$	H → L (45%), H − 1 → L + 1(38%)		
252.55	4.90996	0.0596	$\pi-\pi^*$	H − 1 → L (45%), H → L + 1 (38%)		
232.85	5.32542	0.0001	$\pi-\pi^*$	H → L + 1 (43%), H − 1 → L (40%)		

H: HOMO, L: LUMO.

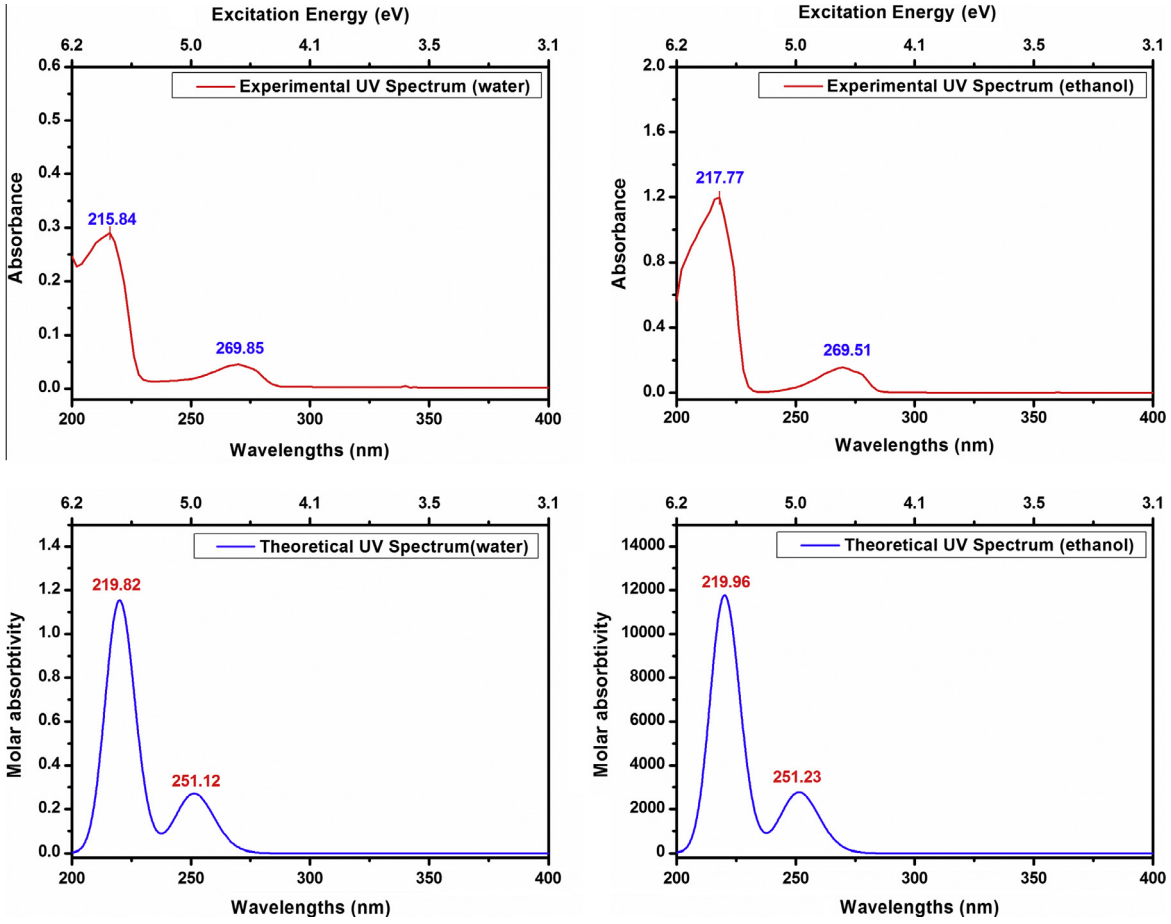

Fig. 9. The experimental and theoretical UV–Vis spectrum of 3,5-DFPBA for ethanol and water solution.

tively the ^{13}C and ^{1}H NMR chemical shifts of the 3,5-DFPBA are described fairly well by the selected DFT method combined with the basis set. There is a good agreement between experimental and theoretical chemical shifts results for the title compound.

To see correlation between the experimental and theoretical total chemical shifts for monomer structure of title molecule were graphed in Fig. 8. ^{1}H NMR values due to the very too little data the correlation seen not good however the values are good agreement for one by one. The relations between experimental chemical shifts (δ_{exp}) and the calculated ones described by the following equations:

$$\text{Total}: \delta_{cal}(\text{ppm}) = 1.0691\delta_{exp} + 0.0468 \quad (R^2 = 0.9935)$$

$$^{1}H: \delta_{cal}(\text{ppm}) = 1.3636\delta_{exp} - 2.7255 \quad (R^2 = 0.3425)$$

$$^{13}C: \delta_{cal}(\text{ppm}) = 1.0043\delta_{exp} + 8.7540 \quad (R^2 = 0.9353)$$

4.5. Electronic properties

4.5.1. UV spectrum and Frontier molecular orbital analysis

The UV spectra analyses of the 3,5-DFPBA were researched by experimental and theoretical calculation for the most stable isomer and its dimer structure. Molecules allow strong $\pi-\pi^*$ and $\sigma-\sigma^*$ transition in the UV–Vis region with high extinction coefficients [84]. The electronic absorption spectrum of title molecule was measured in ethanol and water solution at room temperature. It is obvious that to use TD-DFT calculations to predict the electronic absorption spectra is a quite reasonable method. Because of this the excitation energies, absorbance and oscillator strengths for the title molecule at the optimized geometry in the ground state were obtained in the framework of TD-DFT calculations with the B3LYP/6-311++G(d,p) method. The experimental absorption wavelengths (energies) and computed electronic values, such as absorption wavelength (λ), excitation energies (E), oscillator strengths (f), and major contributions of the transitions and assignments of electronic transitions are tabulated in Table 5.

Moreover, the experimental and theoretical UV spectra of the 3,5-DFPBA are shown in Fig. 9. Experimentally determined maximum absorption values are 215.84 and 269.85 nm in water and 217.77 and 269.51 nm in ethanol, respectively. Theoretically these values are predicted at 199.19, 219.96 and 251.23 nm and 198.92, 219.82 and 251.12 nm in ethanol and water solvents, used TD-DFT/B3LYP/6-311++G(d,p) basis set, respectively. The gas phase values are also calculated nearly 195.99, 208.04 and 252.05 nm so the molecule maybe affected the solvents. These excitations correspond to $\pi-\pi^*$ transition. The calculations are increasing for dimer structure and the major contributions are changing these can be dimeric effect of the molecule.

The most important orbitals in a molecule are the frontier molecular orbitals (FMOs), called highest occupied molecular orbital (HOMO) and lowest unoccupied molecular orbital (LUMO) and very useful for physicists and chemists are the main orbital taking part in chemical reaction. The HOMO (H) energy characterizes the ability of electron giving; LUMO (L) characterizes the ability of electron accepting. The energy of the HOMO is directly related to the ionization potential, while LUMO energy is directly related to the electron affinity [85]. This is also used by the frontier electron density for predicting the most reactive position in π-electron sys-

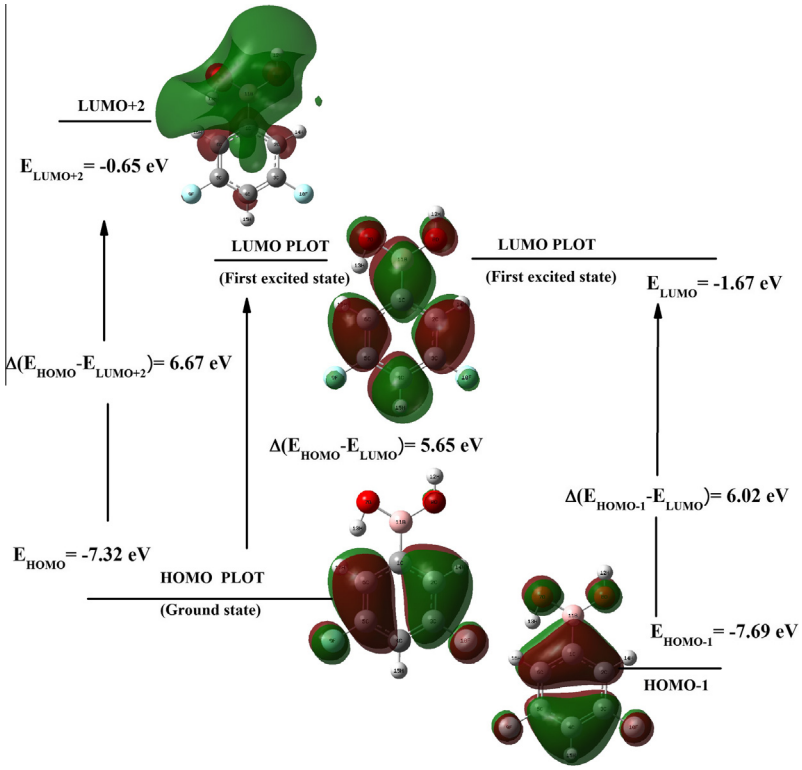

Fig. 10. The frontier molecular orbitals of 3,5-DFPBA for gas phase.

tems and also explains several types of reaction in conjugated system [86]. The conjugated molecules are characterized by a small highest occupied molecular orbital–lowest unoccupied molecular orbital (H–L) separation, which is the result of a significant degree of intra-molecular charge transfer from the end-capping electron-donor groups to the efficient electron-acceptor group through-π-conjugated path [87].

The surfaces of FMOs (HOMO−1, HOMO, LUMO and LUMO+2) are drawn and given in Fig. 10 to understand the bonding scheme of present compound. The HOMO and LUMO energy calculated as −7.32 eV and −1.67 eV for gas phase by TD-DFT method, respectively. The energy gap, difference between H → L, H−1 → L and H → L+2 orbital, is a critical parameter in determining molecular electrical transport properties because it is a measure of electron conductivity. The most important energy gaps (H → L, H−1 → L and H → L+2) were calculated at 5.65 eV, 6.02 eV and 6.67 eV for gas phase for title molecule. These values were also calculated (monomeric and dimeric structures) in two solvents of the title molecule and presented in Table 6. All the HOMO and LUMO have nodes. The nodes in each HOMO−1, HOMO and LUMO are placed nearly symmetrically. However the LUMO+2 of the molecule have no symmetrically nodes. The red and green colors are positive and negative phase, respectively. The HOMO a charge density localized over ring of the entire molecule expect $B(OH)_2$ group, but the LUMO is characterized by a charge distribution on all structure. LUMO+2 the negative (green) nodes located cover the $B(OH)_2$ group due to the electronegative properties of this group. Moreover the energy gap explains the eventual charge transfer interactions taking place within the molecule. The most important energy gaps of the title molecule were given in Fig. 10 and Table 6. Also the contributions of these transitions were computed GaussSum 2.2 [57] and gathered in Table 5 as a major contributions.

Table 6
The calculated energies values of monomer and dimer structures of 3,5-DFPBA molecule using by the TD-DFT/B3LYP method with 6-311++G(d,p) basis set for *ct* conformer.

TD-DFT/B3LYP/6-311++G(d,p)	Monomer			Dimer		
	Gas phase	Ethanol	Water	Gas phase	Ethanol	Water
E_{total} (Hartree)	−606.9317187	−606.9403446	−606.9407442	−1213.878603	−1213.892558	−1213.893223
E_{HOMO} (eV)	−7.32	−7.28	−7.28	−7.38	−7.29	−7.29
E_{LUMO} (eV)	−1.67	−1.59	−1.59	−1.77	−1.62	−1.62
E_{HOMO-1} (eV)	−7.69	−7.62	−7.62	−7.38	−7.29	−7.29
E_{LUMO+1} (eV)	−0.72	−0.67	−0.67	−1.73	−1.59	−1.58
E_{LUMO+2} (eV)	−0.65	−0.34	−0.33	−0.86	−0.68	−0.68
$E_{HOMO-1-LUMO\ gap}$ (eV)	6.02	6.03	6.03	5.61	5.67	5.67
$E_{HOMO-LUMO\ gap}$ (eV)	5.65	5.69	5.69	5.61	5.67	5.67
$E_{HOMO-LUMO+2\ gap}$ (eV)	6.67	6.94	6.95	6.52	6.61	6.61
$E_{HOMO-1-LUMO+2\ gap}$ (eV)	7.04	7.28	7.29	6.52	6.61	6.61
Chemical hardness (h)	2.83	2.85	2.85	2.81	−2.84	−2.84
Electronegativity (χ)	4.50	4.44	4.44	4.58	4.46	4.46
Chemical potential (μ)	−4.50	−4.44	−4.44	−4.58	−4.46	−4.46
Electrophilicity index (ω)	3.58	3.46	3.46	3.73	−3.50	−3.50

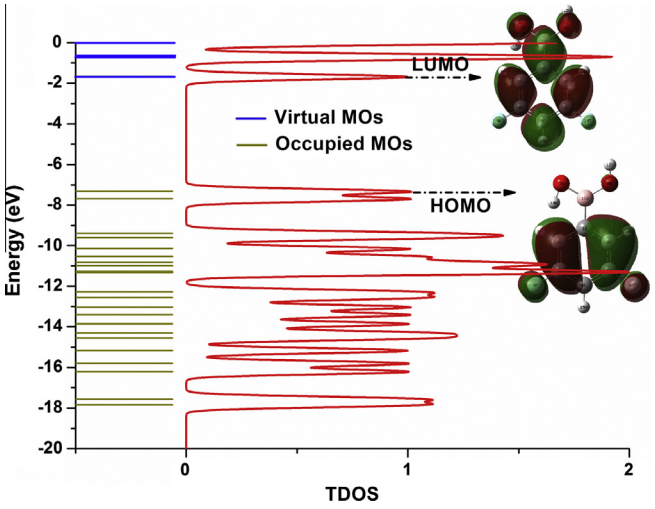

Fig. 11. The calculated total electronic density of states diagram for 3,5-DFPBA.

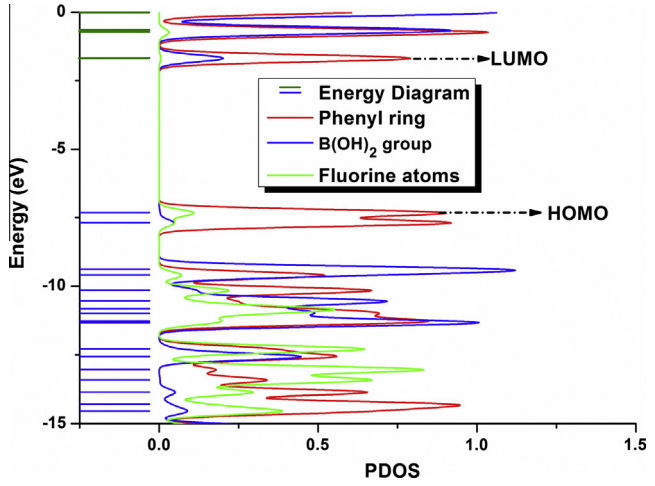

Fig. 12. The calculated partial electronic density of states diagram for 3,5-DFPBA.

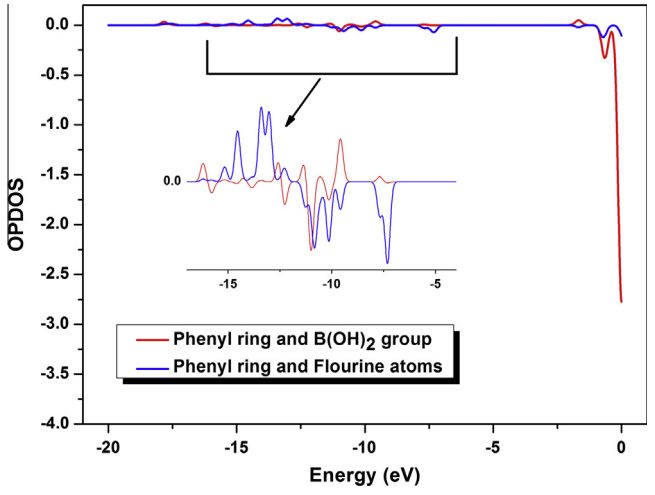

Fig. 13. The overlap population electronic density of states diagrams for 3,5-DFPBA.

The value of chemical hardness is 2.83 eV in gas phase, 2.85 eV in ethanol and water solvents. Also the values of electronegativity, chemical potential and electrophilicity index are different in gas phase and two solvents. These values are given in Table 6.

4.5.2. Total, partial, and overlap population density-of-states

To provide a pictorial representation of (molecule orbital) MO compositions and their contributions to chemical bonding, The TDOS, PDOS, and OPDOS or COOP density of states of the 3,5-DFPBA are plotted in Figs. 11–13, respectively, created by convoluting the molecular orbital information with Gaussian curves of unit height and Full width at half maximum (FWHM) of 0.3 eV using the GaussSum 2.2 program [57]. The most important application of the DOS plots is to demonstrate MO compositions and their contributions to chemical bonding through the OPDOS plots which are also referred in the literature as COOP diagrams. The OPDOS shows the bonding, anti-bonding and nonbonding nature of the interaction of the two orbitals, atoms or groups. A positive value of the OPDOS indicates a bonding interaction (because of the positive overlap population), negative value means that there is an anti-bonding interaction (due to negative overlap population) and zero value indicates nonbonding interactions [88]. Additionally, the OPDOS diagrams allow us to the determination and comparison of the donor–acceptor properties of the ligands and ascertain the bonding, non-bonding. In the boundary region, neighboring orbitals may show quasi degenerate energy levels. In such cases, consideration of only the HOMO and LUMO may not yield a realistic description of the frontier orbitals [89–91].

As seen Fig. 10 HOMO orbitals are localized on C_6H_3 and two fluorine atoms their contributions ca. 100%. The LUMO orbitals are localized on the C_6H_3 and two fluorine atoms (79%) and boronic acid (20%) of the compound. However the OPDOS diagram is shown Fig. 13 and some of orbitals of energy values of interaction between selected groups which are shown from figures easily, phenyl ring ↔ $B(OH)_2$ group (red line) system is positive (bonding interaction) as well as phenyl ring ↔ fluorine atoms (blue line) have bonding and anti-bonding character.

4.5.3. Molecular electrostatic potential surface

The molecular electrostatic potential surface (MEPs) is a plot of electrostatic potential mapped onto the constant electron density surface. The MEPs superimposed on top of the total energy density as a shell. Because of the usefulness feature to study reactivity given that an approaching electrophile will be attracted to negative regions (where the electron distribution effect is dominant). In the majority of the MEPs, while the maximum negative region which preferred site for electrophilic attack indications as red color, the maximum positive region which preferred site for nucleophilic attack symptoms as blue color. The importance of MEPs lies in the fact that it simultaneously displays molecular size, shape as well as positive, negative and neutral electrostatic potential regions in terms of color grading and is very useful in research of molecular structure with its physicochemical property relationship [92,93].

The MEPs of 3,5-DFPBA molecule in 3D plots is illustrated in Fig. 14. The different values of the electrostatic potential at the surface are exemplified by different colors in the map of MEPs. Potential increases in the order from red to blue color. The color code of the maps is between −0.06767 a.u. (dark red) and 0.06767 a.u. (dark blue) in compound, where blue indicates the strongest attraction and red indicates the strongest repulsion. As can be seen from the MEPs map of the title molecule, negative and positive potential regions are localized near OH groups. Namely, the regions having the negative and the positive potential were over the electronegative atom (O_7 and O_8 atoms) and the hydrogen atoms (H_{12} and H_{13} atoms), respectively. If compared, the negative potential value are −0.023081 (O_8 atom) and −0.0196623 (O_7 atom) a.u. for oxygen atoms and the hydrogen atoms also has the negative

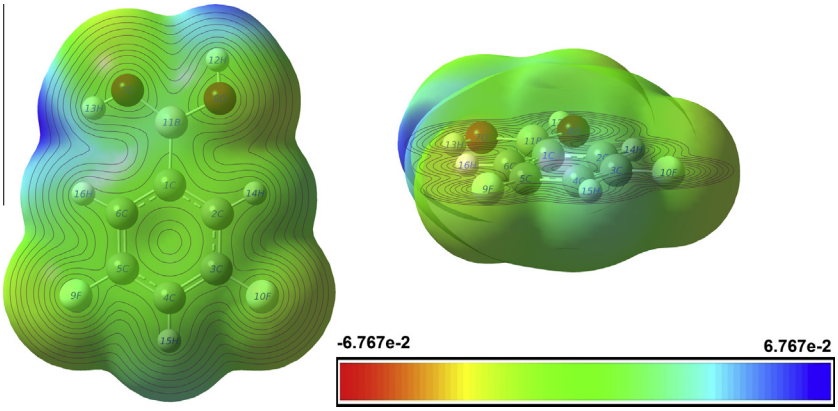

Fig. 14. Molecular electrostatic potential map of 3,5-DFPBA.

potential values are 0.0550337 a.u. (H_{12} atom) and 0.067444 a.u. (H_{13} atom). The O_8 atom has larger negative potential value than the O_7 atom ones. Also H_{13} atom has larger positive potential value than H_{12} atom. From this result, we can say that the H atoms indicate the strongest attraction and O_8 atom indicate the strongest repulsion. The other strongest repulsion showed on the fluorine atoms.

4.5.4. Mulliken atomic charges

Mulliken atomic charges are computed by the DFT/B3LYP method 6-311++G(d,p) basis set. The computed of reactive atomic charges plays an important role in the application of quantum mechanical calculations the molecular system. The Mulliken atomic charges of the 3,5-DFPBA and phenyl boronic acid in Table 7 and shown in Fig. 15. The results show that substitution of the phenyl ring by fluorine atoms and C_4 lead to a redistribution of electron density. Namely, the charges of $B(OH)_2$ groups are same distribution (negative or positive) for two molecules, however, the charge of C_4 of the molecules gives a different charge with each other, is negative in phenyl ring. However, when are added fluorine atoms of the phenyl boronic acid, the values of Mulliken atomic charge of 3,5-DFPBA show negative charge in molecule. Hydrogen atoms exhibit a positive charge, which is an acceptor atom for each one. The boron atom also has more positive charge than the hydrogen atoms because of the substitution of oxygen atoms of the two-hydroxyl groups.

Table 7
Mulliken charges of 3,5-difluoro phenylboronic acid and phenylboronic acid using B3LYP/6-311++G(d,p) basis set.

Atoms	3,5-DFPBA	Phenylboronic acid
C1	−0.811	−0.652
C2	0.488	0.210
C3	−0.826	−0.381
C4	0.770	−0.035
C5	−0.730	−0.326
C6	0.468	0.098
O7	−0.369	−0.342
O8	−0.375	−0.389
F9	−0.167	0.158
F10	−0.168	0.158
B11	0.548	0.533
H12	0.293	0.297
H13	0.233	0.221
H14	0.237	0.191
H15	0.233	0.158
H16	0.177	0.103

4.6. Thermodynamic properties

The thermodynamic parameters (such as zero-point vibrational energy, thermal energy, specific heat capacity, rotational constants, entropy and dipole moment) of monomer and dimer structure of *ct* form, and *tt* and *cc* form of studied molecule were calculated by using DFT/B3LYP/6-311++G(d,p) method at room temperature (298.15 K) in the ground state. The global minimum energy obtained for stable structure (*ct*) optimization of B3LYP with 6-311++G(d,p) basis set as −606.9317187 a.u. (monomer) −1213.878603 a.u. (dimer) and the Zero-Point Vibrational Energies (ZPVEs) as 67.76758 kcal mol^{-1} (monomer) and 136.69393 kcal mol^{-1} (dimer). The other parameters also were listed in Table 8.

To see change of thermodynamic functions (heat capacity, entropy and enthalpy) according to varying temperature for the title molecule the temperature was scanned from 100 K to 700 K, varied every 50 K due to the fact that the molecular vibrational intensities increase with temperature. The obtained thermodynamic functions based on for varied temperature listed in Table 9 according to vibrational analysis. From Table 9, it can be observed that these thermodynamic functions are increasing with temperature. The correlation equations between temperatures and heat capacity, entropy, enthalpy changes were fitted by quadratic formulas and the

Table 8
The calculated thermodynamical parameters of 3,5-DFPBA at 298.15 K for all forms in the ground state at the B3LYP/6-311++G(d,p) level.

Conformers	Cis–Trans (CT)		Trans–Trans (TT)	Cis–Cis (CC)
	Monomer	Dimer	Monomer	Monomer
Symmetry group	C_s	C_1	C_{2v}	C_1
SCF energy (a.u.)	−606.9317187	−1213.878603	−606.9292244	−606.9262675
Zero point vib. energy (kcal mol^{-1})	67.76758	136.69393	−67.64799	−67.9352
Rotational constants (GHz)	1.5019	0.74932	1.49572	1.49573
	0.78347	0.06767	0.7919	0.76794
	0.51488	0.06207	0.51777	0.52442
Specific heat, Cv (cal mol^{-1} K^{-1})	36.368	77.088	36.59	36.182
Entropy, S (cal mol^{-1} K^{-1})	101.069	162.736	95.379	96.617

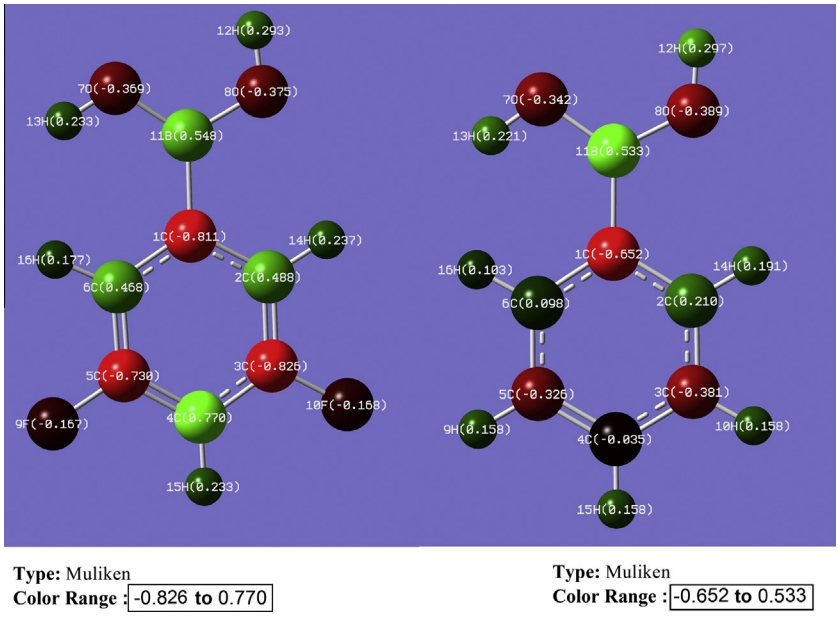

Fig. 15. The Mulliken charge distribution for 3,5-DFPBA.

Table 9
Thermodynamic properties at different temperatures at the B3LYP/6-311++G(d,p) level for 3,5-DFPBA.

T (K)	C (cal mol^{-1} K^{-1})	S (cal mol^{-1} K^{-1})	H (kcal mol^{-1})
100	14.257	73.288	1.198
150	19.856	80.917	2.148
200	25.648	87.995	3.385
250	31.267	94.770	4.908
298.15	36.368	101.069	6.634
300	36.557	101.307	6.705
350	41.421	107.619	8.755
400	45.806	113.708	11.038
450	49.700	119.566	13.527
500	53.130	125.194	16.199
550	56.122	130.591	19.031
600	58.785	135.765	22.005
650	61.115	140.723	25.103
700	63.178	145.477	28.311

corresponding fitting factors (R^2) were obtained as 0.9998, 0.9999 and 0.9997, respectively. The corresponding fitting equations are as follows and the correlation graphics of those shown in Fig. 16.

$$C = -0.03799 + 0.14557T - 7.9161 \times 10^{-5}T^2 \quad (R^2 = 0.9998)$$

$$S = 58.1753 + 0.15802T - 4.7749 \times 10^{-5}T^2 \quad (R^2 = 0.9999)$$

$$H = -0.7153 + 0.01270T + 4.1585 \times 10^{-5}T^2 \quad (R^2 = 0.9997)$$

All the thermodynamic data supply helpful information for the further study on the 3,5-DFPBA. They can be used to compute the other thermodynamic energies according to relationships of thermodynamic functions and estimate directions of chemical reactions according to the second law of thermodynamics in Thermochemical field. Notice: all thermodynamic calculations were done in gas phase and they could not be used in solution.

4.7. Nonlinear optical properties and dipole moment

In this study, the electronic dipole moment, molecular polarizability, anisotropy of polarizability and molecular first hyperpolarizability of present compound were investigated. The polarizability and hyperpolarizability tensors (α_{xx}, α_{xy}, α_{yy}, α_{xz}, α_{yz}, α_{zz} and β_{xxx}, β_{xxy}, β_{xyy}, β_{yyy}, β_{xxz}, β_{xyz}, β_{yyz}, β_{xzz}, β_{yzz}, β_{zzz}) can be obtained by a

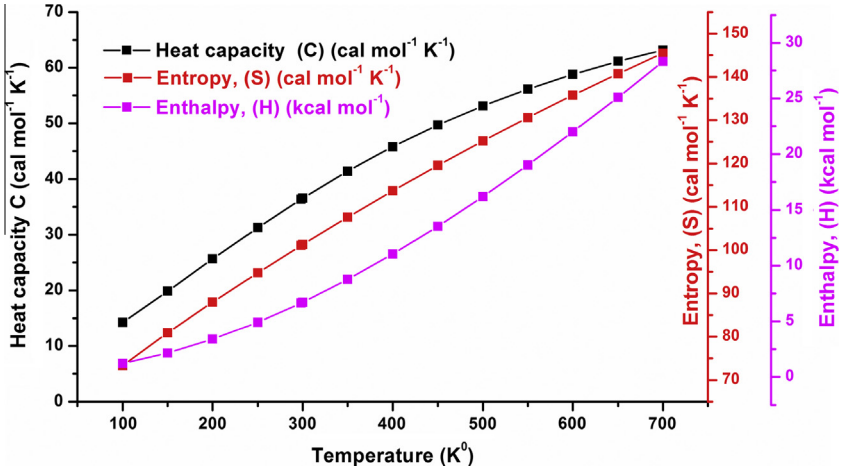

Fig. 16. Correlation graphic of heat capacity, entropy, enthalpy and temperature for 3,5-DFPBA.

Table 10
The dipole moments μ (D), the polarizability α (a.u.), the average polarizability α_o ($\times 10^{-24}$ esu), the anisotropy of the polarizability $\Delta\alpha$ ($\times 10^{-24}$ esu), and the first hyperpolarizability β ($\times 10^{-33}$ esu) of 3,5-DFPBA.

μ_x	1.2104	β_{xxx}	−1298.286145
μ_y	1.4619	β_{xxy}	42.380433
μ_z	0	β_{xyy}	−699.305616
μ_0	1.8979	β_{yyy}	329.511458
α_{xx}	16.943278	β_{xxz}	0
α_{xy}	0.002427	β_{xyz}	0
α_{yy}	14.727152	β_{yyz}	0
α_{xz}	0	β_{xzz}	−119.315005
α_{yz}	0	β_{yzz}	52.893017
α_{zz}	7.478205	β_{zzz}	0
α_{total}	13.049545	β_x	−2116.906766
$\Delta\alpha$	30.573632	β_y	424.784909
		β_z	0
		β	2159.105480

frequency job output file of Gaussian. However, α and β values of Gaussian output are in atomic units (a.u.) so they have been converted into electronic units (esu) (α; 1 a.u. = 0.1482×10^{-24} esu, β; 1 a.u. = 8.6393×10^{-33} esu). The mean polarizability (α), anisotropy of polarizability ($\Delta\alpha$) and the average value of the first hyperpolarizability $\langle\beta\rangle$ can be calculated using the equations.

$$\alpha_{tot} = \frac{1}{3}(\alpha_{xx} + \alpha_{yy} + \alpha_{zz})$$

$$\Delta\alpha = \frac{1}{\sqrt{2}}[(\alpha_{xx} - \alpha_{yy})^2 + (\alpha_{yy} - \alpha_{zz})^2 + (\alpha_{zz} - \alpha_{xx})^2 + 6\alpha_{xz}^2 + 6\alpha_{xy}^2 + 6\alpha_{yz}^2]^{\frac{1}{2}}$$

$$\langle\beta\rangle = [(\beta_{xxx} + \beta_{xyy} + \beta_{xzz})^2 + (\beta_{yyy} + \beta_{yzz} + \beta_{yxx})^2 + (\beta_{zzz} + \beta_{zxx} + \beta_{zyy})^2]^{\frac{1}{2}}$$

In Table 10, the calculated parameters described above and electronic dipole moment {μ_i (i = x, y, z) and total dipole moment μ_{tot}} for title compound are listed. The total dipole moment can be calculated using the following equation.

$$\mu_{tot} = (\mu_x^2 + \mu_y^2 + \mu_z^2)^{\frac{1}{2}}$$

It is well known that the higher values of dipole moment, molecular polarizability, and hyperpolarizability are important for more active NLO properties. 3,5-DFPBA has relatively homogeneous charge distribution and it does not have large dipole moment. The calculated value of dipole moment was found to be 1.8979 Debye. The highest value of dipole moment is observed for component μ_y. In this direction, this value is equal to 1.4619 D and μ_z is the smallest one. The calculated polarizability and anisotropy of the polarizability of 3,5-DFPBA is $13.049545 \times 10^{-24}$ and $30.573632 \times 10^{-24}$ esu, respectively. The magnitude of the molecular hyperpolarizability β, is one of important key factors in a NLO system. The B3LYP/6-311++G(d,p) calculated first hyperpolarizability value (β) of NA is equal to $2159.105480 \times 10^{-33}$ esu. The first hyperpolarizability, polarizability, anisotropy of the polarizability and dipole moment values of 3,5-DFPBA are larger than those of urea.

5. Conclusion

The spectroscopic properties such as molecular parameters, frequency assignments, electronic transitions and magnetic properties of 3,5-DFPBA by using FT-IR, FT-Raman, ^{1}H and ^{13}C NMR and UV–Vis. techniques both experimentally and theoretically. A conformational analysis was carried out by means of DFT. The most stable conformer identified as *ct* form. The vibrational FT-IR and FT-Raman spectra of the 3,5-DFPBA were recorded with experimental and vibrational wavenumbers and their TED were computed. The magnetic properties of the title molecule were calculated and observed in DMSO solution. Some chemical shifts of hydrogen atoms were not observed this may be due to the fluorine atoms and/or DMSO solvent effects. The electronic properties were also calculated and the experimental electronic spectrum was recorded in ethanol and water solution with help of UV–Vis spectrometer. The maxima absorption wavelengths were observed 217.77, 269.51 and 215.84, 269.85 nm in ethanol and water solution, respectively, which these bands are possibly due to the $\pi \rightarrow \pi^*$ transition. The comparison of predicted bands with experimental was done and shows an acceptable general agreement. When all theoretical results scanned, they are showing good correlation with experimental data.

Acknowledgement

This work was supported by the Celal Bayar University Research fund through research Grant No.: FBE-2011/70.

Appendix A. Supplementary material

Supplementary data associated with this article can be found, in the online version, at http://dx.doi.org/10.1016/j.molstruc.2013.10.064.

References

[1] W. Tjarks, A.K.M. Anisuzzaman, L. Liu, S.H. Soloway, R.F. Barth, D.J. Perkins, D.M. Adams, J. Med. Chem. 35 (1992) 16228.
[2] Y. Yamamoto, Pure Appl. Chem. 63 (1991) 423.
[3] F. Alam, A.H. Soloway, R.F. Barth, N. Mafune, D.M. Adam, W.H. Knoth, J. Med. Chem. 32 (1989) 2326.
[4] M.R. Stabile et al., Bioorg. Med. Chem. Lett. 21 (1996) 2501.
[5] P.R. Westmark, B.D. Smith, J. Pharm. Sci. 85 (1996) 266.
[6] N.A. Petasis, Aust. J. Chem. 60 (2007) 795.
[7] E. Cuthbertson, Boronic Acids: Properties and Applications, Alfa Aesar, Heysham, 2006.
[8] A.H. Soloway, R.G. Fairchild, Sci. Am. 262 (1990) 100–107.
[9] D.A. Matthews, R.A. Alden, J.J. Birktoft, S.T. Freer, J. Kraut, J. Biol. Chem. 250 (1975) 7120–7126.
[10] D.H. Kinder, S.K. Frank, M.M. Ames, J. Med. Chem. 33 (1990) 819–823.
[11] X. Chen, G. Liang, D. Whitmire, J.P. Bowen, J. Phys. Org. Chem. 11 (1988) 378–386.
[12] S.J. Rettig, J. Trotte, Can. J. Chem. 55 (1977) 3071–3075.
[13] M.K. Cyrański, A. Jezierska, P. Klimentowska, J.J. Panek, A. Sporzyński, J. Phys. Org. Chem. 21 (2008) 472.
[14] M.R. Shimpi, N.S. Lekshmi, V.R. Pedireddi, Cryst. Growth Des. 7 (10) (2007) 1958.
[15] P.N. Horton, M.B. Hursthouse, M.A. Becket, M.P.R. Hankey, Acta Crystallogr., Sect. E: Struct. Rep. E60 (2004) o2204–o2206.
[16] Y.M. Wu, C.C. Dong, S. Liu, H.-J. Zhu, Y.-Z. Wu, Acta Cryst. E62 (2006) o4236–o4237.
[17] D.C. Bradley, I.S. Harding, A.D. Keefe, M. Motevalli, D.H. Zheng, J. Chem. Soc., Dalton Trans. (1996) 3931–3936.
[18] A. Vega, M. Zarate, H. Tlahuext, H. Höpfl, Acta Cryst. E 66 (2010) o1260.
[19] B. Zarychta, J. Zaleski, A. Sporzynski, M. Dabrowski, J. Serwatowski, Acta Cryst. C60 (2004) o344–o345.
[20] P. Rodríguez-Cuamatzi, G. Vargas-Díaz, T. Maris, J.D. Wuestb, H. Höpfl, Acta Cryst. E60 (2004) o1316–o1318.
[21] P. Rodriguez-Cuamatzi, H. Tlahuext, H. Höpfl, Acta Cryst. E65 (2009) o44–o45.
[22] J.A. Faniran, H.F. Shurvell, Can. J. Chem. 46 (1968) 2089.
[23] Y. Erdogdu, M.T. Gulluoglu, M. Kurt, J. Raman Spectrosc. 40 (2009) 1615–1623.
[24] M. Kurt, J. Mol. Struct. 874 (2008) 159–169.
[25] M. Kurt, J. Raman Spectrosc. 40 (2009) 67–75.
[26] M. Kurt, T.R. Sertbakan, M. Ozduran, M. Karabacak, J. Mol. Struct. 921 (2009) 178–187.
[27] M. Kurt, T.R. Sertbakan, M. Ozduran, Spectrochim. Acta Part A Mol. Biomol. Spectrosc. 70 (2008) 664–673.
[28] S. Ayyappan, N. Sundaraganesan, M. Kurt, T.R. Sertbakand, M. Ozduran, J. Raman Spectrosc. 41 (2010) 1379–1387.
[29] O. Alver, Chimie 14 (2011) 446–455.
[30] O. Alver, C. Parlak, Vib. Spectrosc. 54 (2010) 1–9.
[31] M. Karabacak, E. Kose, A. Atac, M.A. Cipiloglu, M. Kurt, Spectrochim. Acta Part A 97 (2012) 892–908.

[32] M. Karabacak, L. Sinha, O. Prasad, A.M. Asiri, M. Cinar, Spectrochim. Acta Part A 70 (2013).
[33] U. Rani, M. Karabacak, O. Tanrıverdi, M. Kurt, N. Sundaraganesan, Spectrochim. Acta Part A 92 (2012) 67–77.
[34] M.K. Cyrański, A. Jezierska, P. Klimentowska, J.J. Panek, A. Sporzyński, J. Chem. Phys. 128 (2008) 124512.
[35] M. Karabacak, A. Coruh, M. Kurt, J. Mol. Struct. 892 (2008) 125–131.
[36] R.G. Parr, W. Yang, Density Functional Theory of Atoms and Molecules, Oxford, New York, 1989.
[37] W. Kohn, L.J. Sham, Phys. Rev. A 140 (1965) 1133.
[38] R.O. Jones, O. Gunnarson, Rev. Mol. Phys. 61 (1989) 689.
[39] M. Karabacak, Z. Cinar, M. Cinar, Spectrochim. Acta A 79 (2011) 1511–1519.
[40] P.B. Nagabalasubramanian, M. Karabacak, S. Periandy, Spectrochim. Acta A 85 (2012) 43–52.
[41] M. Karabacak, M. Cinar, Spectrochim. Acta A 86 (2012) 590–599.
[42] M. Govindarajan, M. Karabacak, Spectrochim. Acta A 86 (2012) 251–260.
[43] P. Hohenberg, W. Kohn, Phys. Rev. 136 (1964) B864–B871.
[44] A.D. Becke, J. Chem. Phys. 98 (1993) 5648–5652.
[45] C. Lee, W. Yang, R.G. Parr, Phys. Rev. B 37 (1988) 785–789.
[46] M.J. Frisch et al., GAUSSIAN 09, Revision A.1, Gaussian Inc., Wallingford, CT, 2009.
[47] N. Sundaraganesan, S. Ilakiamani, H. Salem, P.M. Wojciechowski, D. Michalska, Spectrochim. Acta A 61 (2005) 2995–3001.
[48] M. Karabacak, M. Kurt, Spectrochim. Acta A 71 (2008) 876–883.
[49] J. Baker, A.A. Jarzecki, P. Pulay, J. Phys. Chem. A102 (1998) 1412–1424.
[50] P. Pulay, J. Baker, K. Wolinski, 2013 Green AcresRoad, Suite A, Fayettevile, AR72703, USA.
[51] R. Ditchfield, J. Chem. Phys. 56 (1972) 5688–5691.
[52] K. Wolinski, J.F. Hinton, P. Pulay, J. Am. Chem. Soc. 112 (1990) 8251–8260.
[53] M. Petersilka, U.J. Gossmann, E.K.U. Gross, Phys. Rev. Lett. 76 (1966) 1212–1215.
[54] E. Runge, E.K.U. Gross, Phys. Rev. Lett. 52 (1984) 997–1000.
[55] R. Bauernschmitt, R. Ahlrichs, Chem. Phys. Lett. 256 (1996) 454–464.
[56] M. Karabacak, M. Cinar, A. Coruh, M. Kurt, J. Mol. Struct. 919 (2009) 26–33.
[57] N.M. O'Boyle, A.L. Tenderholt, K.M. Langner, J. Comp. Chem. 29 (2008) 839–845.
[58] K.L. Bhat, N.J. Howard, H. Rostami, J.H. Lai, Charles W. Bock, J. Mol. Struct. (Theochem) 723 (2005) 147.
[59] C. Par, E.T. Bavoux, P. Michel, Acta Cryst. B 30 (1974) 2043.
[60] N. Sundaraganesan, B. Anand, C. Meganathan, B. Dominic Joshua, Spectrochim. Acta A 68 (2007) 561–566.
[61] A.R. Choudhury, T.N. Guru Row, Acta Cryst. E60 (2004) o1595.
[62] M. Karabacak, E. Kose, M. Kurt, J. Raman Spectrosc. 41 (2010) 1085–1097.
[63] L.J. Bellamy, The Infrared Spectra of Complex Molecules, Wiley, New York, 1959.
[64] D. Sajan, I. Hubert Joe, V.S. Jayakumar, J. Zaleski, J. Mol. Struct. 785 (2006) 43–45.
[65] M. Silverstein, G. Clayton Basseler, C. Morill, Spectrometric Identification of Organic Compounds, Wiley, New York, 2001.
[66] V. Arjunan, I. Saravanan, P. Ravindran, S. Mohan, Spectrochim. Acta A 74 (2009) 375–384.
[67] G. Varsanyi, Assignments of Vibrational Spectra of Seven Hundred Benzene Derivatives, vol. 1–2, Adam Hilger, 1974.
[68] C.N.R. Rao, Chemical Applications of Infrared Spectroscopy, Academic Press, New York, 1959.
[69] G. Socrates, Infrared and Raman Characteristic Group Frequencies, John Wiley, New York, 2001.
[70] N.A. Narasimham, M.Z. El-Saban, J. Rud-Nielson, J. Chem. Phys. (USA) 24 (1956) 420.
[71] E.E. Ferguson et al., J. Chem. Phys. (USA) 21 (1953) 1464.
[72] A.K. Ansari, P.K. Verma, Spectrochim. Acta A 35 (1979) 35.
[73] M.S. Navati, M.A. Shashindhar, Ind. J. Phys. 66B (1994) 371.
[74] N. Sundaraganesan, S. Ilakiamani, B. Dominic Joshua, Spectrochim. Acta A 67 (2007) 287–297.
[75] D. Mahadevan, S. Periandy, M. Karabacak, S. Ramalingam, Spectrochim. Acta A 82 (2011) 481–492.
[76] S.H. Brewer, A.M. Allen, S.E. Lappi, T.L. Chase, K.A. Briggman, C.B. Gorman, S. Franzen, Langmuir 20 (2004) 5512.
[77] V. Krishnakumar, V. Balachandran, Spectrochim. Acta, A 61 (2005) 1001.
[78] B. Stuart, Infrared Spectroscopy: Fundamentals and Applications, Wiley India Ed., 2010.
[79] G. Kahraman, O. Beskarcles, Z.M. Rzave, E. Piskin, Polymer 45 (2004) 5813.
[80] L. Santucci, H. Gilman, J. Am. Chem. Soc. 80 (1958) 193–196.
[81] N. Subramania, N. Sundaraganesan, J. Jayabharathi, Spectrochim. Acta A 76 (2010) 259–269.
[82] H.O. Kalinowski, S. Berger, S. Braun, Carbon-13 NMR Spectroscopy, John Wiley & Sons, Chichester, 1988.
[83] K. Pihlaja, E. Kleinpeter (Eds.), Carbon-13 Chemical Shifts in Structural and Sterochemical Analysis, VCH Publishers, Deerfield Beach, 1994.
[84] F.A. Cotton, C.W. Wilkinson, Advanced Inorganic Chemistry, third ed., Interscience Publisher, New York, 1972.
[85] S. Gunasekaran, R.A. Balaji, S. Kumeresan, G. Anand, S. Srinivasan, Can. J. Anal. Sci. Spectrosc. 53 (2008) 149.
[86] K. Fukui, T. Yonezawa, H. Shingu, J. Chem. Phys. 20 (1952) 722.
[87] C.H. Choi, M. Kertesz, J. Phys. Chem. 101A (1997) 3823.
[88] M. Chen, U.V. Waghmare, C.M. Friend, E. Kaxiras, J. Chem. Phys. 109 (1998) 6680–6854.
[89] R. Hoffmann, Solids and Surfaces: A Chemist's View of Bonding in Extended Structures, VCH Publishers, New York, 1988.
[90] T. Hughbanks, R. Hoffmann, J. Am. Chem. Soc. 105 (1983) 3528.
[91] J.G. Małecki, Polyhedron 29 (2010) 1973.
[92] J.S. Murray, K. Sen, Molecular Electrostatic Potentials, Concepts and Applications, Elsevier, Amsterdam, 1996.
[93] E. Scrocco, J. Tomasi, in: P. Lowdin (Ed.), Advances in Quantum Chemistry, Academic Press, New York, 1978.